FINITE ELEMENT MODELING OF THE ELASTOPLASTIC BEHAVIOR OF MULTILAYER METALLIC COMPOSITES

by

© Yasmeen Shoker

A Thesis submitted to the

School of Graduate Studies

in partial fulfillment of the requirements for the degree of

Master of Engineering

Faculty of Engineering & Applied Science

Memorial University of Newfoundland

October 2021

St. John's Newfoundland

ABSTRACT

The aerospace industry has long favored lightweight materials to optimize fuel efficiency. The use of lightweight materials poses stringent requirements on enhancing aircraft structures in harsh environmental conditions. This in turn prompted many investigations on using cladded and multilayer materials as a potential solution for corrosive environments. Recent interest has been garnered in cladding for its adequate corrosion resistance without significantly compromising cost and performance. To date, the evaluation of these multilayer composite structures is normally established through laboratory testing of small-scale specimens. However, understanding the structural performance of cladded composites can be better accomplished using numerical simulations via finite element analysis (FEA). Utilizing FEA simulation enables the application of the derived knowledge of material properties and elastoplastic behavior to larger-scale structures. This study employs FEA to predict the behavior of cladded materials in the elastic-plastic region. In particular, ABAQUS commercial FEA software is used to model these metals' elastoplastic behavior. Increased precision is achieved by calibrating and comparing the generated stress-strain data obtained from these simulations with experimental measurements. A mesh convergence study is employed to determine the adequate mesh size. Ultimately, the FEA models for individual metals are used to predict the mechanical response of multilayer materials in the elastoplastic region. Simulation results are in close agreement with their corresponding experimental counterparts, further confirming the model's accuracy and effectiveness. The Ramberg-Osgood (R-O) relationship is employed to reveal closely matching curves that are within

close proximity of the experimental and modeled responses at several heat-treated temperatures. Additionally, a parametric study that investigates different cladding scenarios and how they can potentially yield enhanced tensile strength and ductility by optimizing their required cladding thickness is completed. The viability of optimizing a bilayer composite's elastoplastic behavior based on exploring varying combinations of bilayer composites, materials, and thicknesses is also discussed. This research is significant for two reasons: it yields a profound understanding of multilayer materials mechanical performance, and it introduces a FEA simulation technique that enables structural and design optimization of larger-scale structures to effectively fulfill design requirements.

ACKNOWLEDGEMENTS

This thesis is the product of my research conducted at Memorial University of Newfoundland. Working on this thesis has taught me firsthand that research cannot simply be measured in terms of success or failure, but rather the amount of gained experiences that lead to furthering technical skills along with an increased depth of understanding. The potential of meaningful work is often masked with setbacks which collectively provide an opportunity for more rigorous and all-encompassing technical solutions.

I would like to thank my research supervisor, Dr. Sam Nakhla to whom I owe a great debt of gratitude for his generous insight and valuable expertise which has been instrumental to the completion of this thesis. I would also like to extend my thanks to the late Dr. Shirokoff, who was one of my co-supervisors when I first started my graduate program. His knowledge and discussions will be remembered with great prominence. I would also like to express my thanks to Dr. Ahmed Elruby for allocating his time to help with the technical software components of this thesis which has led to the procurement of meaningful technical analysis that could prove useful to other inquisitive researchers in years to come.

I would also like to express my gratitude to Memorial University of Newfoundland and Bombardier Inc. for providing the resources and financial support that has made this work possible.

Table of Contents

ABSTRACT ..... *ii*

ACKNOWLEDGEMENTS ..... *iv*

Table of Contents ..... *v*

List of Tables ..... *viii*

List of Figures ..... *ix*

List of Symbols, Nomenclature or Abbreviations ..... *x*

1 Introduction and Literature Review *1*

1.1 Background 1

1.2 Literature Review 3

1.2.1 Introduction 3

1.2.2 Mechanical properties 4

1.2.3 Uniaxial tensile testing theory 5

1.2.4 Review of the stress and strain relationship 7

1.2.5 Deformation and strain energy 9

1.2.6 Ramberg-Osgood Relationship 12

1.2.7 Plastic deformation of polycrystalline materials 14

1.2.8 Cladding 14

1.2.9 Interfacial layers between metals 16

1.2.10 Experiments involving cladding and bi/tri-layer materials 18

1.3 Thesis Overview and Purpose 22

1.4 Co-authorship Statement 24

1.5 References 26

2 FE Simulation to Extract Tensile Deformation Characteristics of the Individual Component Metals and Model Verification 29

2.1 Introduction 29

2.2 Stress-strain response of prismatic specimen under uniaxial tensile loading 30

2.3 Purpose 30

2.4 Simulation Overview 31

2.4.1 Model geometry and overview 31
2.4.2 Material calibration 32
2.5 Description of Experimental Benchmark and Model Validation 33
2.5.1 Modeling separate materials and comparing their stress-strain response to experimental data available in the literature 33
2.5.2 Validating the model's accuracy through experimental and simulated mechanical property comparison of a bi-layered Al/STS clad composite 34
2.5.3 Simulation results of a bi-layered Al/STS clad composite 36
2.5.4 Contour profiles at select increments 38
2.5.5 Implementation of the model to simulate the individual component tensile deformation characteristics of a tri-layered composite 40
2.6 Comparisons of Simulation and Experimental Behaviors 43
2.7 Ramberg-Osgood parameters 44
2.8 Conclusions 47
2.9 References 50

3 FEA of the Elastoplastic Behavior of Multilayered Clad Composites *52*
3.1 Introduction 52
3.2 Modeling Procedure for Composite Material Assembly 52
3.3 Simulation Results and Discussion 54
3.4 Mesh convergence study for Al3003-STS439 clad composite 55
3.5 Comparisons of Simulation and Experimental Behaviors 61
3.6 Conclusions 62
3.7 References 63

4 Modeling Composite Candidates: A Parametric Study *64*
4.1 Introduction 64
4.2 Modeling the Behavior of Clad Composite Candidates 64
4.2.1 Candidate 1: MgAZ31/SST430 Clad Composite 65
4.2.2 Candidate 2: Al3004/SST430 Clad Composite 65
4.3 Clad Composite Candidates Discussion and Comparisons 65
4.4 Conclusions 67

4.5 References 68

5 Summary and Conclusions *69*
5.1 Summary 69
5.2 Contributions 69
5.3 Recommendations for Future Work 70

List of Tables

Table 1. Comparison of experimental and simulated yield and tensile properties 44
Table 2: R-O parameters of experimental and modeled stress-strain responses of Al 3003 at various temperatures 46
Table 3: R-O parameters of experimental and modeled stress-strain responses of STS 439 at various temperatures 47
Table 4. Summary of simulated and testing mechanical responses 61
Table 5. Summary of yield strength and ultimate strength of composite candidates 66

List of Figures

Figure 1. Schematic stress-strain curve 7
Figure 2. Prismatic bar under uniaxial loading 8
Figure 3. The increase in length of a specimen under a uniaxial tensile applied load .9
Figure 4: Example of a bi-layer composite consisting of two separate layer sheets 15
Figure 5. Example of a tri-layer composite consisting of three separate layer sheets 15
Figure 6. Specimen geometry for single material modeling 32
Figure 7. Layered sheet arrangement and dimensions of tensile test specimen used by Jin and Hong (2013) 34
Figure 8. Simulated and experimental stress-strain responses of heat treated the Al3003 sheet at 500°C for 1hr 37
Figure 9. Simulated and experimental stress-strain responses for the Stainless Steel 439 sheet at 500°C for 1hr 38
Figure 10: Three-dimensional Cauchy stress tensor components 39
Figure 11: STS 439 stress-strain curve and typical contour profile in S22 direction of specimen 39
Figure 12. Arrangement and dimensions of layered plates: AZ31 Mg/3004 Al/SST 430 used by Kim and Hong (2013) 40
Figure 13. Simulated and experimental stress-strain responses for the Al 3004 sheet at 673°K for 3 hrs. 41
Figure 14. Simulated and experimental stress-strain responses for the Stainless Steel 430 sheet at 673°K for 3 hrs. 42
Figure 15. Simulated and experimental stress-strain responses for the Magnesium AZ31 sheet at 673°K for 3 hrs. 43
Figure 16: Comparison of the R-O and testing stress-strain curves of Steel 439 at 400C 46
Figure 17. Modeled geometry of Al3003/STS439 and Mg AZ31/Al3004/SST430 clad composites 53
Figure 18. Simulated and testing engineering stress-strain response comparison for Al3003/STS439 clad composite. 55
Figure 19: Stress-strain responses of mesh convergence study at mesh sizes of 0.5 mm, 1 mm, and 1.5 mm 56
Figure 20. Comparison of modeled and simulated engineering stress-strain responses of individual and combined materials within the composite 57
Figure 21. Simulated and testing stress-strain response comparison of Al3004/MgAZ31/SST430 composite 58
Figure 22. Simulated and testing stress-strain response comparison of Al3004/MgAZ31/SST430 composite and individual component materials 60
Figure 23. Comparative stress-strain responses of composite candidates 66

List of Symbols, Nomenclature or Abbreviations

A	Area
Al	Aluminum
ASTM	American Society for Testing and Materials
DSA	Dynamic Strain Aging
E	Modulus of Elasticity
F	Applied Load
FEA	Finite Element Analysis
FEM	Finite Element Model
FLDs	Forming Limit Diagrams
l_f	Fracture Length
l_o	Original Gauge Length
SEM	Scanning Electron Microscopy
STS	Stainless Steel
ε	Strain
ΔL	Change in Length
σ	Stress
v	Poisson's Ratio
σ_y	Yield Strength
σ_{ul}	Ultimate Strength

1 Introduction and Literature Review

1.1 Background

Multi-layered composites have garnered significant research interest from several industries over the last few decades. Cladded composites are desirable owing to their enhanced mechanical strength and accompanying multifunctional characteristics. Developing these composites consists of bonding two or more materials with dissimilar mechanical properties to fulfill its intended application within its environment efficiently. The extensive selection of existing materials affords substantial design versatility that has inspired numerous research contributions into component material configurations. The motivation for examining the mechanical properties of composites is to predict performance under different loading conditions. Knowledge of composite behavior allows researchers to determine the feasibility of adopting the composite for a given application. Bonded material interfaces are investigated to understand how the materials interact with their neighboring layer within the composite. An interfacial layer may form an oxide layer depending on the nature of the metals in contact. The thickness of the newly created bonding layer could either enhance or hinder the composite's performance. The main aspects considered when designing multilayer composites include component materials, their stacking sequence, corresponding thicknesses, and their interfacial structure. These aspects can be modified in conjunction with the nature of the intended application. For instance, the Bombardier super-scooper comprises of aluminum because it is subject to corrosive environments.

Titanium and steel-clad composites are often used for marine, petrochemical, and constructional purposes because they offer low-cost solutions that withstand high temperatures and adequately perform in highly corrosive environments. The component materials each contribute their advantages; the titanium effectively protects against corrosion while the steel layer provides excellent structural strength (Ha and Hong 2015). Composites containing aluminum, magnesium, and steel have been previously considered for applications that require lightweight materials with the ultimate goal of reducing fuel consumption costs. Cladding steel and aluminum with magnesium has been researched to combat magnesium's poor corrosion resistance. Studies on the aluminum-magnesium interface revealed a protective surface oxide layer that aids in protecting against corrosion (Kim and Hong 2013).

The elastoplastic behavior, such as the yield and tensile strength of composites, generally falls somewhere between their component materials. That being said, the elastoplastic behavior of the overall composite differs from that of its contributing materials. In recent years, researchers have been investigating several techniques to understand the elastoplastic behavior of composites. Yilamu et. al, (2009) explored the springback and bending properties of two and three-ply sheet composites due to their pertinence in sheet metal forming industries. Kang et. al, 2005 investigated two sequences of a five-ply aluminum and steel composite to determine the influence of sequence arrangement and strain rate on mechanical strength. Keun and Ig (2017) considered the impact of residual stress-strain on bending properties using a copper/aluminum/copper clad sequenced plate. Their findings reveal that this composite displayed a higher ductility level than that of

aluminum alone. Aghchai et. al (2008) employed both an experimental and analytical approach to determine that the formability limit of a two-layer composite demonstrates improved forming limit diagrams (FLDs) compared to a single sheet with low formability.

1.2 Literature Review

1.2.1 Introduction

Materials selection is the process of selecting a material that best fits the intended purpose of the engineering application. A wealth of research has been dedicated to study the material properties in engineering design. The design and development of materials with predetermined mechanical properties suitable for the intended function and cost constraints while guaranteeing structural performance. The selected material conforms to all design objectives and constraints to serve its required purpose without experiencing premature mechanical failure. Existing materials are commonly used to develop composites that suit their indented use based on a set list of key objectives and constraints. For instance, steel is often used to reinforce bridges and buildings because of its strength and durability. It can carry heavy loads in tension, compression, and shear without failing. Whereas aluminum alloys are often used in the aerospace industry owing to their low density, good formability, and high specific strength. Aluminum can sustain heavy loads based on its weight despite its lower tensile strength compared to more dense materials like steel, which is ideal for lightweight applications. One of the most essential

aircraft design constraints is limiting the weight as much as possible to limit the costs associated with fuel consumption (Young and Hong, 2013).

Materials are generally classified by their chemical composition and atomic structure and grouped into four main categories: metals, ceramics, polymers, and composites (Callister and Rethwisch, 2010). This thesis's scope focuses mainly on composites, which are two or more combined individual materials from the mentioned categories. Composites are extensively used in designs because they combine additional properties and characteristics taken from each of their component materials. Several material selection optimization software programs exist to determine which materials or existing composite deliver the best fit based on its intended function. However, designing a new composite requires extensive engineering analysis, which is discussed in **Section 2** of this thesis.

1.2.2 Mechanical properties

Mechanical properties are an essential aspect to consider when designing structures because they are the foundation of material candidate selection. These properties pave the understanding for material failure under any given circumstance. Materials are manufactured or designed to ensure structural integrity within service conditions. Several fundamental mechanical properties are discussed below because they are the framework for design integrity in cladded composites. Knowledge of these properties ensures all service requirements are met without the onset of excessive deformation or premature fracture. Mechanical behavior is a term often used to describe how materials perform under applied loads or forces. Mechanical properties are determined mostly through standardized laboratory testing techniques such as the American Society for Testing and

Materials (ASTM) standards to reflect the material's in-service behavior. The laboratory experiments mimic service conditions by reproducing the same category of applied loads (tensile, shear, compressive, etc.), duration (consistent or fluctuating), and environmental conditions.

1.2.3 Uniaxial tensile testing theory

When considering a material for a particular design, engineers often use tensile tests to determine the material's ability to withstand a predetermined amount of uniaxial stress. The purpose of a tensile test is to determine the mechanical properties of a material to allow for more informed designing decisions. Uniaxial tensile tests are often used to determine material parameters such as yield strength, ultimate strength, Young's modulus, Poisson's ratio, ductility, resilience, toughness, and elongation. The tests involve placing a rectangular or circular specimen in a machine with a load cell, extensometer, and moving crosshead. The specimen is stretched (usually referred to as elongated) at a constant rate until fracture while measuring the specimen's elongation with respect to its instantaneous uniaxial applied load in the longitudinal direction as shown in **Figure 1**.

In particular, a specimen is subject to an applied axial load at a constant extension rate until failure. This type of testing method is labeled as destructive because the specimen becomes damaged and can no longer be used. The output load versus elongation curve obtained from the test is dependent on the geometrical parameters and is termed the engineering stress-strain curve. True stress-strain curves are then derived by normalizing these load versus elongation curves to achieve facilitated design flexibility (based on their independence to geometric parameters). Alternate laboratory tests conducted to determine

stress-strain relationships include compression tests and shear and torsional tests. These tests are usually conducted if the material is subjected to in-service forces that resemble compression or shear (Callister and Rethwisch, 2010). From this point forward, all mentions of stress-strain indicate engineering stress-strain.

Mathematical modeling using finite element analysis (FEA) software requires a thorough understanding of stress and strain relationships. Predicting stresses and stress distribution along a structure's members can also be accomplished using theoretical and mathematical finite element stress analyses. Modeling can be accomplished using the aid of a commercially available finite element software such as Abaqus or Ansys. Designing materials using theoretical methods requires knowledge of stress-strain relationships because they provide a gateway into the material's mechanical properties. Stress-strain behavior reveals how a given structure or member will deform under any amount of applied stress. It is first essential to gain a brief understanding of the elastic and plastic regions that make up the stress-strain curve. The simplest way to describe a material's behavior is by illustrating its significant mechanical properties with a schematic diagram of a stress-strain curve.

1.2.4 Review of the stress and strain relationship

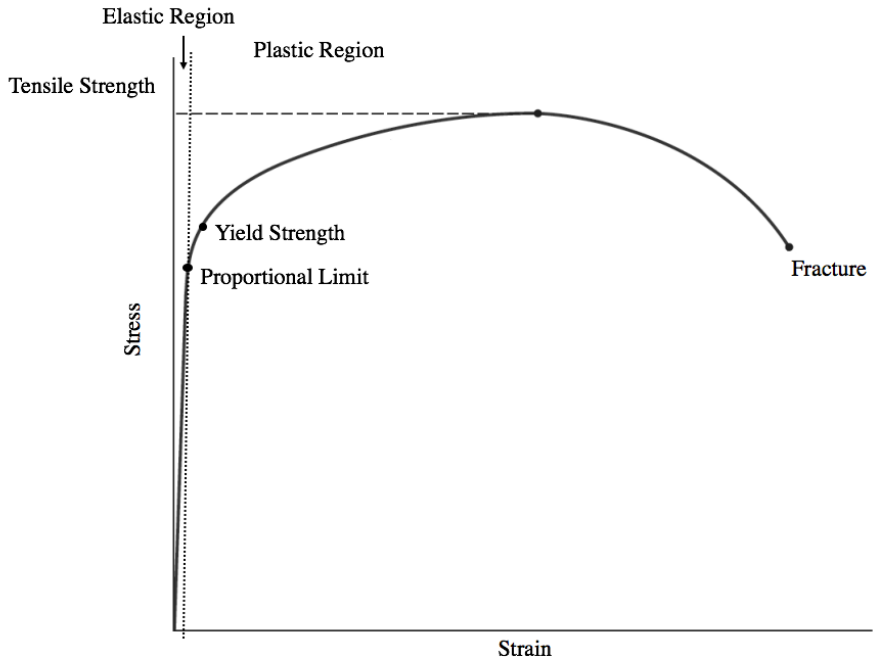

Figure 1. Schematic stress-strain curve

As illustrated in **Figure 1**, a material experiences linear elastic behavior until it reaches a maximum yield strength, after which deformation is no longer linear, and Hooke's law becomes invalid. Once the material's elongation stretches past the yield strength, the stress-strain behavior becomes non-linear and plastic deformation ensues. For this reason, it is imperative to determine the yield point and consider this crucial mechanical property when modeling and simulating deformation to ensure the material can serve its intended purpose up to an acceptable and preset level strain.

Continuing along the engineering stress-strain curve, the remaining mechanical properties experimentally determined by the tensile test include the ultimate tensile strength and fracture point. Plastic deformation continues to a maximum point on the curve called the

tensile strength, after which the curve decreases until fracture. The explanation for the decreasing curve from the tensile strength to fracture point is due to necking. Before the onset of necking, the specimen experiences uniform elongation, but once necking occurs, the specimen's elongation mostly occurs within the localized necking area. Now that the concept of a stress-strain curve has been illustrated using a schematic diagram, the mathematical relationships can now be explained. As shown in **Figure 2**, an applied longitudinal load will subject materials to elastic and plastic deformation. In the elastic region, the relationship of load and elongation demonstrates linear behavior on the stress-strain curve. A member experiencing an axial load causes normal stress in the elastic region.

Figure 2. Prismatic bar under uniaxial loading

The normal stress, σ, can be calculated by dividing the force, F, over the original cross-sectional area, A, using the following relationship:

$$\sigma = \frac{F}{A} \qquad \textbf{(Eq.1.1)}$$

The units of stress are usually expressed in terms of (MPa).

Strain, ε, is expressed as the normalized elongation of a specimen, a member's change in length, divided by its original length. **Figure 3** shows a specimen's increase in length due to an applied load.

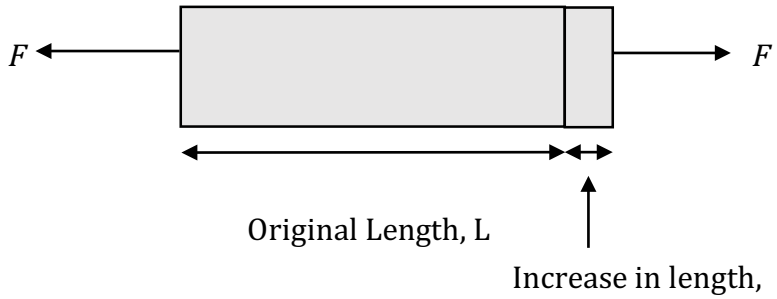

Figure 3. The increase in length of a specimen under a uniaxial tensile applied load

For a prismatic specimen, the normal strain relationship can be defined as:

$$\varepsilon = \frac{\Delta L}{L} \qquad \textbf{(Eq.1.2)}$$

1.2.5 Deformation and strain energy

Several mathematical relationships are used to represent object deformation and fracture principles. Referring to the branch of continuum mechanics, the deformable solid material is assumed to be a continuous medium, described as a displacement of its points shifting to a different location within space. Materials display different elastic behaviors based on their grouping category. The stretching of polymer chains causes elastic responses in polymers. Elastic responses in metals depend on the changes in shape and size of the atomic lattice. For isotropic materials in the elastic region, Hooke's law can represent the relationship between stress and strain. Hooke's law states that the relationship between

stress and strain is directly proportional. The equation to represent this relationship is derived from the relationship between stress and strain tensors below:

$$\sigma = \begin{bmatrix} \sigma_{xx} \\ \sigma_{yy} \\ \sigma_{zz} \\ \sigma_{xy} \\ \sigma_{yz} \\ \sigma_{xz} \end{bmatrix} = \frac{E}{(1+v)(1-v)} \begin{bmatrix} 1-v & v & v & 0 & 0 & 0 \\ v & 1-v & v & 0 & 0 & 0 \\ v & v & 1-v & 0 & 0 & 0 \\ 0 & 0 & 0 & \frac{1}{2}-v & 0 & 0 \\ 0 & 0 & 0 & 0 & \frac{1}{2}-v & 0 \\ 0 & 0 & 0 & 0 & 0 & \frac{1}{2}-v \end{bmatrix} \begin{bmatrix} \varepsilon_{xx} \\ \varepsilon_{yy} \\ \varepsilon_{zz} \\ 2\varepsilon_{xy} \\ 2\varepsilon_{yz} \\ 2\varepsilon_{xz} \end{bmatrix} \quad \textbf{(Eq.1.3)}$$

For a uniaxial stress, **Equation 1.3** simplifies to

$$\sigma = E\varepsilon \quad \textbf{(Eq.1.4)}$$

where σ represents the stress tensor vector, E is the modulus of elasticity, E, the elasticity matrix, ε denotes the strain tensor and v is Poisson's ratio. Hooke's law can only be applied within the Elastic region, where materials experience nonpermanent or elastic deformation. According to Hooke's law, materials in the elastic region have a linear relationship because stress and strain are directly proportional. In the elastic region, deformation exists only under an applied load; therefore, releasing the applied load will allow the structure to return to its original shape after a given time, depending on the material's anelasticity. The E in Hooke's law denotes the modulus of elasticity, commonly referred to as Young's modulus, which ranges between 45 to 407 GPa for most metals (Materials Science and Engineering, 8th Edition). The modulus of elasticity is an essential mechanical property and can be easily calculated by taking the slope of the linear elastic line from the engineering stress strain curve. The relationship of elastic parameters can also be used to determine Poisson's ratio, v, using the following formula,

$$E = 2G(1 + v) \quad \textbf{(Eq.1.5)}$$

where G is around 0.4 E for most metals.

The yield strength, σ_y can be mathematically determined by dividing the yield load, F_y, by the specimen's original cross-sectional, A_o.

$$\sigma_y = \frac{F_y}{A_o} \quad \textbf{(Eq.1.6)}$$

The ultimate tensile strength, σ_{TS} can be found by dividing the maximum load, F_{max}, by the specimen's original cross-sectional area.

$$\sigma_{TS} = \frac{F_{max}}{A_o} \quad \textbf{(Eq.1.7)}$$

Additionally, ductility can be tabulated once fracture occurs. In short, ductility is the percentage of plastic strain at failure and is expressed as the percent elongation using the following formula:

$$\%EL = \frac{l_{f-}l_0}{l_0} \times 100 \quad \textbf{(Eq.1.8)}$$

where l_f denotes fracture length and l_0 represents the original length of the gauge.

The displacement of the specimen can be denoted using the following equation:

$$\Delta L = \frac{FL}{EA} \quad \textbf{(Eq.1.9)}$$

which states that the displacement is directly proportional to the applied load and length of the specimen, and inversely proportional to the specimen's cross-sectional area, and the elastic modulus of the material.

1.2.6 Ramberg-Osgood Relationship

The Ramberg-Osgood Relationship (R-O) is an empirical model that describes the non-linear behavior of a stress-strain curve by employing three parameters: Young's modulus and two secant yield strengths (Ramberg and Osgood, 1943). The original R-O strain deformation equation is:

$$\varepsilon = \frac{\sigma}{E} + K\left(\frac{\sigma}{E}\right)^{\frac{1}{n}} \quad \textbf{(Eq.1.10)}$$

where ε denotes strain, σ is stress, E is Young's Modulus, while K and n are material dependent constants that describe the material hardening behavior. The premise of this relationship assumes that a straight line can define the elastic section of the curve ε_e, while a power law can model that of the plastic section, ε_p. The total strain is the sum of the elastic and plastic strain components, signified as:

$$\varepsilon = \varepsilon_e + \varepsilon_p \quad \textbf{(Eq.1.11)}$$

The relationship between K is described in the following equation by the adding the parameters of α and σ_0.

$$\alpha = K\left(\frac{\sigma_0}{E}\right)^{n-1} \quad \textbf{(Eq.1.12)}$$

Rewriting the original equation to include a yield offset, α gives

$$\varepsilon = \frac{\sigma}{E} + \alpha * \frac{\sigma}{E}\left(\frac{\sigma}{\sigma_0}\right)^{n-1} \quad \textbf{(Eq.1.13)}$$

Although the Ramberg-Osgood relationship began in the field of engineering and materials science, its focus has evolved to include several diverse and multidisciplinary applications. Since the R-O relationship is material dependent, it has gained attention

from biomedical scientists studying bone fracture. Bone is a material that experiences plasticity prior to fracture, directing researchers to investigate its behavior using uniaxial tensile tests. Sharma et al. (2019) successfully employed the R-O relationship to determine the stress-strain behavior of cortical bone plasticity.

Elruby and Nakhla (2019) extended the Ramberg-Osgood relationship to account for porosity since it significantly influences the material's stress-strain response. They contributed a significant extension to the R-O relationship to illustrate the influence of porosity on mechanical behavior. To better understand their proposed relationship parameters, the R-O equation for uniaxial state of stress is first introduced as

$$E\varepsilon = \sigma + \alpha\sigma\left(\frac{|\sigma|}{\sigma_y}\right)^{n-1} \quad \textbf{(Eq.1.14)}$$

where σ is the uniaxial stress, and σ_y denotes the yield stress.

Their function builds on the previous equation to account for the porosity factor of a given material, which in turn delivers accurate analytical predictions. Their derived porosity factored extended R-O equation introduces new parameters to yield the function

$$Ee^{-mp}\varepsilon = \sigma + \alpha\sigma(\left(\frac{|\sigma|}{\sigma_y e^{-mp}}\right)^{n-1} \quad \textbf{(Eq.1.15)}$$

where p is the volumetric porosity factor and m can be calibrated through micromechanical modeling or testing data. Extensive testing was performed coupled with investigating literature data to support the accuracy of their proposed relationship, which was found to contribute superior analytical capabilities.

1.2.7 Plastic deformation of polycrystalline materials

Deformation at the microstructural level translates to external forces distorting the grain boundaries primarily due to slip and twinning. Before deformation, grains more or less hold equal dimensions in all directions along the specimen. Since grain boundaries remain closed during deformation because of mechanical integrity, the grains culminate in forming new shapes based on the constraints posed by neighboring grains. Considering the majority of the grain boundaries exclusively remain intact, the overall size of the grain does not change, only its shape. Particularly, a specimen extending due to an external force equates to the grain elongating in the same direction as the force. Several strengthening mechanisms exist to reduce deformation by hindering grain dislocation mobility. These mechanisms which aim to increase strength and hardness include grain size reduction, solid-solution strengthening, and strain hardening.

1.2.8 Cladding

Clad metals are composite materials that combine multilayer sheets of metals using various techniques, namely roll bonding or press forming. Cladding combines favorable mechanical properties from dissimilar materials, which has proven to be a unique solution when designing multi-functional materials. Cladding generally involves pairing a weaker material with a thin layer of a stronger material to improve its mechanical performance and simultaneously overcome low ductility. Mechanical joining of the materials into a composite usually involves a roll bonding process such as hot roll bonding or roll-cladding. Once the composite is bonded together, it undergoes a heat treatment process to strengthen the bonding and increase the ductility and interfacial layers between the

materials. The most common cladded products feature a stainless steel (STS) and aluminum (Al) composite. STS contributes corrosion resistance and high strength, while Al provides the benefit of being lightweight. (Kang et al. 2006). These properties are often desirable in the aerospace industry because they alleviate costs associated with fuel consumption. **Figures 4 and 5** show composites consisting of two and three contributing material layers, respectively. These materials can be re-arranged to investigate which configurations provide the most optimal behavior.

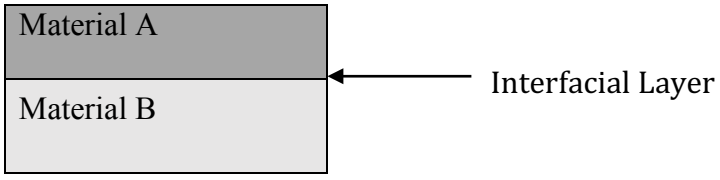

Figure 4: Example of a bi-layer composite consisting of two separate layer sheets

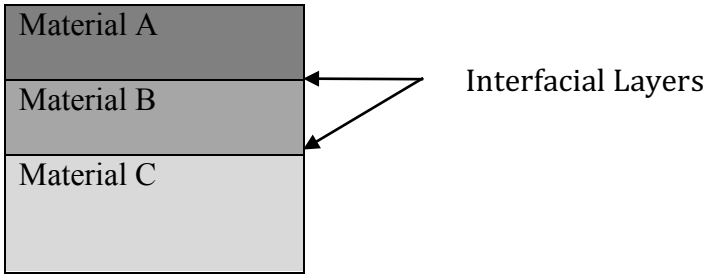

Figure 5. Example of a tri-layer composite consisting of three separate layer sheets

The effects of temperature and strain rate are often considered when attempting to optimize the ultimate tensile strength and formability of multilayer clad composites. Stress-strain curves are used to provide insight into how the strain rate influences mechanical strength. These curves reveal stress humps at varying temperature locations depending on the strain rate. Although increasing the temperature to intermediate levels

for metals such as titanium and steel grants higher strength, the tradeoff is decreased ductility due to dynamic strain aging (DSA) due to carbon present within the steel. However, increasing the strain rate improves ductility within higher temperature ranges up to a maximum temperature, after which the ductility decreases. Elongation has shown to be higher in low strain rates at higher temperature levels (above 300°C). Increased ductility is attributed to homogeneous deformation and limiting localized necking in one of the component layers (Ha and Hong, 2013). Aghchai et al. (2208) employed both an experimental and theoretical approach to determine that the formability of a two-layer metallic sheet displays better forming limit diagrams (FLDs) than that of a single component sheet. The FLD curves determined analytically were found to be in close agreement with those obtained experimentally.

1.2.9 Interfacial layers between metals

Compared to a single material, modeling a composite requires more complexity due to the potential presence of interfacial layers between the metal sheets. A composite material consisting of layered sheets does not always behave as a single material because slight or detrimental interfaces may form, which contain vulnerabilities such as shear stresses that can cause the layer's bonded surface to become brittle, and thus more susceptible to debonding (Kim and Hong, 2013, Ha and Hong, 2015). Warping can also occur in tensile specimen composites due to transverse stresses that arise from the different plastic strain ratios of the component materials (Choi et al., 1997). Studies have found that increasing the thickness of intermetallic compounds increases with temperature (Keun and Ig, 2017).

Understanding how these interfacial layers contribute to the overall design of cladded materials gives rise to more accurate modeling methods.

Manufacturing processes cause imperfections in interlayers of composites. Fractures can form on the metallic surface caused by mismatched rotational speeds during an asymmetrical bonding process. Inter-diffusion of the component layers can also trigger the development of an interlayer on the interface (Li et al., 2013). Wrinkling behavior within the multilayer sheets resulting from excessive metal flowing into the die cavity during the process of deep drawing heavily influences failure within sheet metals (Morovvati et al., 2010).

The influence of a clad material's interfaces presents several clues into the mechanical performance of a composite. The interface between layers is surveyed for any interfacial cracks, flaws, or reaction layers to factor into the results. For instance, intermetallic layers can originate in composites from being exposed to heat treatment at temperatures higher than the material's ideal strain hardening temperature. For instance, magnesium requires a lower strain hardening temperature compared to steel. However, this composite would have a higher overall mechanical strength if strain hardening is tailored to steel's ideal temperature despite the consequence of forming a reaction layer. (Kim and Hong, 2013). Also, stainless steel experienced a bumpy surface, which was determined to suggest a homogeneous uniform deformation and consequent enhancement in ductility within the clad composite's steel layer.

A reaction layer between magnesium and steel was seen in Kim and Hong's (2013) optical micrograph images at temperatures above 573°K. The interfacial reaction layer

presented undesirable consequences because the reaction compounds obstructed the bonding strength in between the composite's layers. Knowing how the advantages outweigh the disadvantages are worth considering when selecting heat treatment temperatures for the composite.

Once a layer is separated from the composite, researchers have the option to subject it to an annealing process to prevent temperature-dependent intermetallic formation on the sheet's surface properties to enhance the accuracy of results. Furthermore, annealing also improves interfacial bonding (Li et al., 2013). Studies have been performed to take advantage of these interfacial layers by deliberately wanting an intermetallic compound to form on a layer's interface to improve tensile properties and layer bonding. Li et al. (2013) investigated enhanced mechanical strength attributed to interfacial improvement of a laminated aluminum copper clad composite.

The influence of strain rate on deformation behavior revealed that increasing the strain rate enhances the ultimate tensile strength and elongation, and reduces the overall deformation due to the formation of an interfacial layer between the component materials. Hong and Ha, 2017 also considered designing a mechanical bonding interlayer to increase strength in a copper titanium steel clad composite. The purpose of designing an interlayer was to increase the bonding strength and provide good deformability with a low melting temperature. (Hong and Ha, 2013)

1.2.10 Experiments involving cladding and bi/tri-layer materials

The deformation and fracture behavior of several bi-layered and tri-layered clad composites have been studied extensively. Most researchers have concluded that cladding

provides a wide range of new mechanical properties (Kang et al., 2006, Kim and Hong, 2013). Several metals have been considered for cladding layers, such as magnesium and various aluminum and steel alloys. Hong and Kim (2013) looked into the deformation and fracture behavior of roll-bonded magnesium, aluminum, and stainless still clad composite. Although magnesium triggers thoughts of unpromising results owing to its low corrosion resistance attributed to its lack of protective oxide film, it does provide the benefit of being incredibly lightweight, which is something the aerospace industry values significantly. These researchers innovated a compelling composite arrangement ensemble to compensate for magnesium's shortcomings. A magnesium layer was strategically added with aluminum and stainless steel to limit its high corrosion susceptibility. Cladding aluminum with magnesium yields Al_2O_3, a protective surface oxide layer that effectively guards against corrosion. As an effort to optimize the composite, a thin layer of steel was added due to its high mechanical strength and to compensate for the lack of corrosion resistance in magnesium.

Each component material contributes its mechanical properties to the overall composite, meaning the fracture strain of the entire composite should theoretically be influenced by each material's strength contributions. Kim and Hong (2013) provided evidence to confirm this claim, using a series of tensile tests to determine their composite's strain at failure. They carried out several tension tests on tri-layered hot roll bonded composites Mg/Al/SST, under varying degrees of heat treatment. Composites were separated, and tests were conducted on each material to determine each material's individual mechanical properties. The reasoning for testing the materials separately and combined is to

determine each material's strength and ductility contribution towards the overall composite. The practice of comparing the stress-strain curves of the combined and individual materials delivers a method of verification into the accuracy of the tests. Elaborating on this point, the mechanical properties of the individual materials have already been studied extensively in the past and should therefore fall into a predetermined behavior margin. For instance, the stress-strain curve of steel outputs a higher ultimate tensile strength than aluminum and magnesium.

Additionally, steel's modulus of elasticity is higher than the other two and should reveal a steeper slope in the elastic region. The individual materials' predictable behavior provides a gateway into knowing that the acceptable mechanical behavior of a composite should fall in between its other materials' stress-strain curves. Consequently, the composite's stress-strain curves should exhibit fluctuations when altering the ratio of each material's cross-sectional area. Optical microscopy and scanning electron microscopy (SEM) are used to investigate the microstructure at each interface region and determine whether the bonding surface was intact. Moreover, the ultimate purpose of these images is to investigate the occurrence of homogeneous deformation.

Multiple heat treatment temperatures (as rolled and 473°K-673°K) were compared to illustrate the influence of heat treatment on mechanical properties, namely ductility, hardness, and strength. The reasoning for conducting tests at low and high temperatures is due to the concept of recovery and recrystallization. Recrystallization allows materials to have increased fracture strains. A noteworthy property of magnesium is its low recrystallization temperature. A low recrystallization temperature means that magnesium

will experience recrystallization in the lower temperature range, meaning that it shows an increased fracture strain at lower temperatures than higher ones.

Their experiment revealed no benefit in terms of mechanical properties for using this particular cladding composition. The main reasoning was the strength of the Al layer significantly impaired the material's overall strength. However, it was determined that cladding SST with Mg is potentially beneficial because it would be lightweight with improved corrosion resistance. Magnesium contributes the low density, while Stainless Steel provides added corrosion resistance to compensate for magnesium's susceptibility to corrosion.

The details surrounding the composite's strain at failure is perhaps the most notable finding of their experiment. Increasing the heat treatment temperature also increased the total fracture strain of the composite once the Mg alloy fractured, even though higher heat treatment temperatures decrease the fracture strain of Mg alloys. This is due to the Al/SST contributing to a higher fracture strain after the increased heat treatment temperature. Therefore, the localized deformation of the Mg layer does not play a part in decreasing the enhanced ductility of the composite since the remaining layers were well bonded.

Other studies have looked into incorporating more than two or three materials into a composite. Kang et al. (2006) investigated a five-ply stainless-steel aluminum composite's strain behavior. Kang et al. (2006) investigated roll bonding's influence on mechanical properties based on material thickness and arrangement using textural measurements and a finite element method that encompasses friction conditions. The

crystallographic texture and strain rate variations caused by distinct texture gradients were analyzed in the roll-gap. Their results revealed that the composite's material arrangement presents a notable impact on the strain rates. Regardless of the material, the mid sheet of the composite underwent significant and uniform plain strain deformation. It was also determined that strain history plays a vital role in the rise of deformation, mainly dependent on geometry and the roll bite's friction conditions.

Yilamu et al. (2009) investigated the role stainless-steel clad aluminum plays on air bending characteristics and springback phenomena. Uniaxial tension tests were conducted to determine the mechanical properties of the individual materials and the hot-rolled aluminum/steel sheet sandwich. The stress-strain curve showed the composite curve to sit in between the steel and aluminum curves as anticipated. This curve explains how the clad sheet has a mechanical strength proportional to the combined components from a behavior standpoint. The strength of the composite is higher than aluminum and less than steel. The arrangement of the materials dramatically influences V-bending angles, but play a minor role in springback. The composite possessing the stronger material layer in the inside position causes a decrease in the composite's overall thickness and a smaller bending angle and radius than the opposite case. The springback can be accurately depicted using the Yoshida-Uemori model to simulate clad sheet metal springback behavior because it considers the Bauschinger effect (Yilamu et al., 2009).

1.3 Thesis Overview and Purpose

Although there have been significant theoretical and experimental contributions to determine the mechanical behavior of composites, most of the existing research is

restricted to small-scale specimens. There is little in the way of translating derived mechanical behaviors from a small-scale specimen to a larger scale. This evident gap in the literature merits a closer look. This research proposes to bridge this inherent gap by implementing a finite element model that can represent and accurately predict large-scale composites' material behavior. The purpose of this thesis is to contribute a finite element model that grants the potential to accurately grasp the mechanical behavior of composites via virtual tensile tests. Simulating theoretically intensive tensile tests using a quantified computer model which outputs accurate and verifiable mechanical properties contributes several advantages compared to laboratory testing. First and foremost, costs associated with laboratory equipment and resources are reduced. A wide array of versatile feasibility studies can be simulated to determine the ideal contributing material sequence and thickness without accumulating associated testing costs.

Determining the material properties of composites was achieved by designing a model in Abaqus CAE that simulates tensile tests and generates output stress-strain curves to reveal key mechanical properties. Consistent with prior research practices, individual stress-strain responses are established for the composite and each of its contributing materials. The model's accuracy is verified through a series of tensile test simulations that generated material stress-strain responses in close agreement with those of testing. The model's simulated mechanical behavior for a particular material closely matches that of testing. This thesis consists of four chapters, each building on the former to provide a more profound understanding of the model's advantages and feasibility. The first chapter consists of an introduction, literature review, and purpose of work. The second chapter

introduces the model's design and methodology for extracting mechanical properties such as tensile and yield strength from individual contributing materials within a composite. This chapter focuses exclusively on simulating stress-strain responses of individual materials within the composite and then comparing the simulated output response to that of testing to support and verify the model's accuracy. The Ramberg-Osgood (R-O) relationship is used to determine and compare the experimental and simulated (n-1) and α variables. The third chapter provides the methodology of designing a composite within Abaqus. The simulated stress-strain response of the whole composite is then compared to that of testing. The fourth chapter discusses the conclusions and limitations of the model. A parametric study that predicts the behavior of a newly designed composite using previously obtained mechanical properties is presented to demonstrate the feasibility of using this model in future research.

1.4 Co-authorship Statement

I, Yasmeen Shoker (YS), hold primary author status for all chapters in this thesis. The following authors have aided with the development of the thesis: Dr. Sam Nakhla (SN) and Dr. Ahmed Elruby (AE). Work from this thesis has been presented at the CSME 2021 conference, in addition to the making of a journal paper (pending submission). Regarding the conceptualization, visualization and methodology, [SN and AE] contributed their knowledge and expertise. The supervision oversight, project administration, leadership, resources, review of results was made possible by [SN and AE]. The contribution of advice and knowledge regarding the formal analysis methodology, software support and

reviewing results was aided by [AE and SN]. This statement applies to all chapters in this thesis. Funding acquisition by [SN].

1.5 References

Aghchai, A Jalali, Shakeri, M, and Mollaei-Dariani, B. "Theoretical and Experimental Formability Study of Two-layer Metallic Sheet (Al1100/St12)." Proceedings of the Institution of Mechanical Engineers. Part B, Journal of Engineering Manufacture 222.9 (2008): 1131-138.

Callister and Rethwisch. "Materials Science and Engineering an Introduction 8th Edition", John Wiley and Sons, Inc., (2010): 45-79, 151-174, 198-210.

Choi, Shi-Hoon, Kim, Keun-Hwan, Oh, Kyu Hwan, and Lee, Dong Nyung. "Tensile Deformation Behavior of Stainless Steel Clad Aluminum Bilayer Sheet." Materials Science & Engineering. A, Structural Materials: Properties, Microstructure and Processing 222.2 (1997): 158-65.

Elruby, Ahmed Y, and Nakhla, Sam. "Strain Energy Density Based Damage Initiation in Heavily Cross-linked Epoxy Using XFEM." Theoretical and Applied Fracture Mechanics 103 (2019): 102254.

Ha, Jong Su, and Hong, Sun Ig. "Deformation and Fracture of Ti/439 Stainless Steel Clad Composite at Intermediate Temperatures." Materials Science & Engineering. A, Structural Materials : Properties, Microstructure and Processing 651 (2016): 805-09.

Ha, Jong Su, and Hong, Sun Ig. "Design of High Strength Cu Alloy Interlayer for Mechanical Bonding Ti to Steel and Characterization of Their Tri-layered Clad." Materials in Engineering 51 (2013): 293-99.

Hambli, Ridha, and Reszka, Marian. "Fracture Criteria Identification Using an Inverse Technique Method and Blanking Experiment." International Journal of Mechanical Sciences 44.7 (2002): 1349-361.

Hong, Sun Ig, and Kim, Yong Keun. "Residual Stress/Strain Effect on the Bending Properties of the Cu/Al/Cu Clad Plate." Key Engineering Materials 737 (2017): 214-19.

Jalali Aghchai, A, Jalali Aghchai, A, Shakeri, M, Shakeri, M, Mollaei Dariani, B, and Mollaei Dariani, B. "Influences of Material Properties of Components on Formability of Two-layer Metallic Sheets." International Journal of Advanced Manufacturing Technology 66.5 (2013): 809-23.

Jin, Ju Young, and Hong, Sun Ig. "Effect of Heat Treatment on Tensile Deformation Characteristics and Properties of Al3003/STS439 Clad Composite." Materials Science & Engineering. A, Structural Materials : Properties, Microstructure and Processing 596 (2014): 1-8.

Kang, H.G, Kim, J.K, Huh, M.Y, and Engler, O. "A Combined Texture and FEM Study of Strain States during Roll-cladding of Five-ply Stainless Steel/aluminum Composites." Materials Science & Engineering. A, Structural Materials : Properties, Microstructure and Processing 452 (2007): 347-58.

Kim, In-Kyu, and Hong, Sun Ig. "Roll-Bonded Tri-Layered Mg/Al/Stainless Steel Clad Composites and Their Deformation and Fracture Behavior." Metallurgical and Materials Transactions. A, Physical Metallurgy and Materials Science 44.8 (2013): 3890-900.

Li, Xiaobing, Zu, Guoyin, and Wang, Ping. "Effect of Strain Rate on Tensile Performance of Al/Cu/Al Laminated Composites Produced by Asymmetrical Roll Bonding." Materials Science & Engineering. A, Structural Materials : Properties, Microstructure and Processing 575 (2013): 61-64.

Morovvati, Mohammad Reza, Morovvati, Mohammad Reza, Fatemi, Afshin, Fatemi, Afshin, Sadighi, Mojtaba, and Sadighi, Mojtaba. "Experimental and Finite Element Investigation on Wrinkling of Circular Single Layer and Two-layer Sheet Metals in Deep Drawing Process." International Journal of Advanced Manufacturing Technology 54.1 (2011): 113-21.

Oya, Tetsuo, Tiesler, Nicolas, Kawanishi, Seiichiro, Yanagimoto, Jun, and Koseki, Toshihiko. "Experimental and Numerical Analysis of Multilayered Steel Sheets upon Bending." Journal of Materials Processing Technology 210.14 (2010): 1926-933.

Ramberg, Walter, and William R. Osgood. "Description of stress-strain curves by three parameters." (1943).

Sharma, N. K, Sarker, M. D, Naghieh, Saman, and Chen, Daniel X. B. "Studies on the Stress-Strain Relationship Bovine Cortical Bone Based on Ramberg–Osgood Equation." Journal of Biomechanical Engineering 141.4 (2019): Journal of Biomechanical Engineering, 2019-04-01, Vol.141 (4).

Tseng, Huang-Chi, Tseng, Huang-Chi, Hung, Chinghua, Hung, Chinghua, Huang, Chin-Chuan, and Huang, Chin-Chuan. "An Analysis of the Formability of Aluminum/copper Clad Metals with Different Thicknesses by the Finite Element Method and Experiment." International Journal of Advanced Manufacturing Technology 49.9 (2010): 1029-036.

Yilamu, K, Hino, R, Hamasaki, H, and Yoshida, F. "Air Bending and Springback of Stainless Steel Clad Aluminum Sheet." Journal of Materials Processing Technology 210.2 (2010): 272-78.

Zhu, Deju, Mobasher, Barzin, Rajan, S. D, and Peralta, Pedro. "Characterization of Dynamic Tensile Testing Using Aluminum Alloy 6061-T6 at Intermediate Strain Rates." Journal of Engineering Mechanics 137.10 (2011): 669-79.

2 FE Simulation to Extract Tensile Deformation Characteristics of the Individual Component Metals and Model Verification

2.1 Introduction

Cladding dissimilar metals show significant promise to enhance the mechanical performance of a structure. Designing composites comprising of materials with diverse mechanical properties provides the advantage of multifunctional applications coupled with reduced costs. Investigating the mechanical behavior is imperative to determine a composite's limitations within its intended environment. Extensive laboratory experimental testing has been conducted on metal composites, triggering the potential of accumulating significant costs over time. Repetitive testing consumes both time and resources despite the advantages. In this sense, providing a cost-efficient solution to determine the mechanical properties of composites is critical. Numerical modeling approaches have the potential to mitigate existing financial constraints while providing high-quality results. Finite element modeling is the standard universal numerical modeling method used for structural analysis. Finite element modeling (FEM) is a numerical solution that approximates the behavioral response of an object by creating a mesh of smaller elements. A FEM which simulates mechanical behavior by generating stress-strain responses would efficiently provide accurate results in an inexpensive and timely manner. Before the composite's behavior can be predicted, the stress-strain response of its component metals must be investigated to authenticate the model's validity.

2.2 Stress-strain response of prismatic specimen under uniaxial tensile loading

The stress-strain curve describes the elastic and plastic material behavior under a uniaxial tensile force. As previously mentioned, the elastic and plastic regions are separated by the material's yield point. The elastic region obeys Hooke's Law, stating that the stress is proportional to strain, whereas stresses in the plastic region inflict permanent plastic deformation. From a microstructural viewpoint, plastic deformation is the result slip, which involves atomic grain boundary dislocation motions. The specimen's deformation is uniform prior to the ultimate point, after which the deformation filters to a certain point along the specimen and forms a neck. The formation of a neck, whose cross-sectional area continues to decrease with applied force due to the confined deformation at the neck is known as the necking phenomenon. If the applied stress continues, the neck will continue to elongate until a resulting fracture occurs at some point along the neck. The stress at failure is defined as the specimen's fracture strength.

2.3 Purpose

This chapter's intended purpose is to utilize an analytical technique to determine the tensile deformation behavior of the individual component materials of a composite. The current work provides a three-dimensional finite element model that virtually simulates tensile tests to investigate the mechanical properties of lone material. Simulated tensile deformation characteristics are then compared with testing results collected from available literature to verify the model's accuracy so that it may be extended further to predict the mechanical behavior of multi-layered clad composites.

2.4 Simulation Overview

2.4.1 Model geometry and overview

Capturing the elastoplastic mechanical behavior of single materials was achieved by developing a FEM in Abaqus CAE. The modeled geometry comprises of a rectangular prism part with width and length dimensions of 25 mm and 110 mm respectively. Two five-millimeter length-wise partitions were defined, one on each the top and bottom as shown in **Figure 6**. A constant thickness of 10 mm was used for each separate material, as shown in **Figure 6**. Since 10 mm of the specimen is tied up in partitions, only the remaining length of 100 mm is considered when operating on x-y data to generate stress-strain responses. A mesh size of 1.25 mm was found to provide adequate results based on the mesh convergence study, details of which can be found in **Section 3.4**. Once all parts of the specimen are created, Abaqus allows the option of defining material properties that can be assigned to any or all parts of the specimen. The FEM consists of a 3D element with two boundary conditions: fixed and moving. These boundary conditions are the reference points for the force-displacement and stress-strain responses for any given single material and cladded composite. The fixed boundary condition has a symmetry/antisymmetric/encastre type, with a dynamic and explicit step and a uniform distribution. The moving boundary condition has a displacement/rotation type, with a dynamic and explicit step. Material properties are then defined to an assigned section by calibrating testing stress-strain responses. The testing response data is input as a behavior comprising of an elastic-plastic parameter data set, allowing for the tabulation of the

ultimate and yield points. **Figure 6** illustrates the Specimen geometry used for single material modeling.

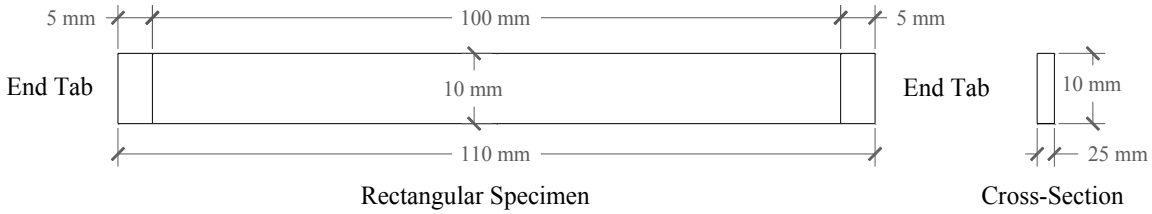

Figure 6. Specimen geometry for single material modeling

2.4.2 Material calibration

Abaqus can develop material behaviors using imported material test data sets. The calibration feature is advantageous because it allows Abaqus to derive material behaviors, namely elasticity, and plasticity. Abaqus tabulates these values by calculating properties such as Young's modulus and Poisson's ratio from imported stress-strain curves. The calibration feature is advantageous because it allows Abaqus to define material behaviors such as elasticity and plasticity easily.

Several stress-strain curves from published work were imported into Abaqus as data sets. This calibration process allows Abaqus to calculate Young's modulus and yield strength from the data sets, allowing more precision for the model's stress-strain response.

2.5 Description of Experimental Benchmark and Model Validation

2.5.1 Modeling separate materials and comparing their stress-strain response to experimental data available in the literature

In this section, experimental tensile deformation characteristics taken from Jin and Hong's (2013) tensile tests are compared to the model's simulated results. The laboratory tensile test was conducted on a 2-ply Al3003/STS439 clad metal sample with thicknesses of 1 mm and 0.5 mm for aluminum and steel, respectively, as illustrated in **Figure 7**. The tensile testing specimen possessed a width of 2.5 mm, and a length of 15 mm. The composite was heat-treated at 500°C for 1hr. The FEM's dissimilar specimen geometry has no influence and does not hinder the accuracy of its output engineering stress-strain response when comparing it to that of a response obtained through testing. The reasoning of which is rooted in the analytical calculations to derive stress. Stress values were obtained manually by dividing the reaction force output of the model by the cross-sectional area of the test specimen, thereby confirming the feasibility of applying this technique. The following section will analytically demonstrate the concept of different geometries by comparing the testing stress-strain response determined by Jin and Hong (2013) to that of the FEM.

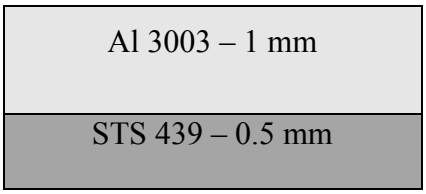

Figure 7. Layered sheet arrangement and dimensions of tensile test specimen used by Jin and Hong (2013)

2.5.2 Validating the model's accuracy through experimental and simulated mechanical property comparison of a bi-layered Al/STS clad composite

Jin and Hong's conducted three experimental tensile tests: one for each contributing material and another for the combined material composite. The resulting stress-strain responses afford important information on material behavior. Based on constraints associated with the scope of this thesis, only the elastic-plastic region of the response is considered. The experimental tensile tests generated three engineering stress-strain curves: aluminum 3003, stainless steel 439, and the aluminum 3003/stainless steel 439 composite. Each material's engineering stress-strain curve was considered up until the stainless steel's ultimate point, at a strain value of approximately 0.11. The reasoning for stopping at the ultimate point of stainless steel was that steel showed lower strain values than aluminum at the ultimate strength. More specifically, the stress-strain curves for both aluminum and steel stop at the same point, which is steel's ultimate strain value of 0.11 as previously mentioned.

The aluminum and steel curves were converted into true stress-strain curves and input into Abaqus as a data set. The engineering stress-strain curve was converted to that of a

true stress-strain curve by manipulating each data point along the curve using **Equations [2.1]** through **[2.3]. Equation [2.2]** expresses the true strain, e, as the natural log of the final length, l_f, of the specimen after being acted on by a tensile force divided by its initial length, l_i.

$$e = ln\left(\frac{l_f}{l_i}\right) \quad \textbf{(Eq.2.1)}$$

Further manipulation of **Equation [2.1]** allows the true strain, e, to be expressed in terms of engineering strain, ε, using the following expression.

$$e = ln\frac{l_i+\Delta l}{l_i} = ln\,(1+\varepsilon) \quad \textbf{(Eq.2.2)}$$

where Δl denotes the change of length of length of the specimen. Similarly, true stress can be obtained from knowledge of the engineering stress using the following equation:

$$\sigma_T = \frac{P}{A_0}(1+e) = s \times (1+e) \quad \textbf{(Eq.2.3)}$$

where σ_T is the true stress, P is the load, A_0 is the initial cross-sectional area and s is the engineering stress. The true stress-strain data for each material was used as input data sets for material calibrations. The aforementioned modeled geometry was used to simulate responses for aluminum and steel individually. First, the elastic behavior for each material was defined, after which the true-stress data was used within the material calibration tool to define the plastic behavior. The material properties were defined using the behavior of each material from the calibration step. Two reference points were added, one at each end tab. The next step was from the interaction module, where constraints were defined at

each end tab. The end tabs are defined as a ridged body and each constraint to the reference points. The boundary conditions are defined in the load module, where the top reference point is permitted to extend in the Y direction while the bottom reference point is fixed.

The output for the reaction force and the displacement in the Y direction at the moving reference point 2 were obtained. The force and displacement were then converted to stress-strain by dividing the force by the cross-sectional area and the displacement by the modeled specimen's gauge length. The reaction force was divided by 25, the model's cross-sectional area, while the displacement was divided by 100, the model's gauge length. It should be noted that these values obtained from the model are engineering stress-strain because the undeformed cross-sectional dimensions were used. This allowed the engineering stress-strain response of the model to be compared with that of testing. Reiterating from **Section 2.3**, the model geometry can be extended to any specimen geometry and provide meaningful comparisons at any given cross-sectional area.

2.5.3 Simulation results of a bi-layered Al/STS clad composite

Figure 8 shows that the model's simulated output stress-strain curve for an Aluminum 3003 sheet is in close agreement with those of testing. **Figure 9** shows the testing and simulated stress-strain responses of Steel 439 are also similar. The fact that the model's stress-stress strain response for both materials are in close agreement to those of testing confirms that the material definitions are deemed acceptable and can thus be extended to further model the composite metal. The combined material composite responses will be discussed in **Chapter 3**.

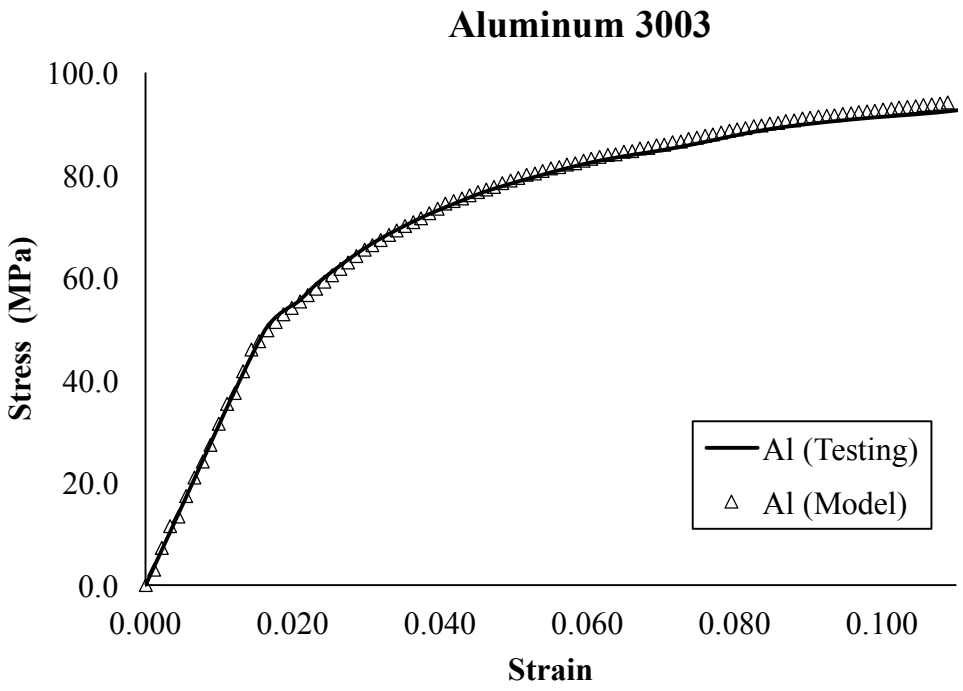

Figure 8. Simulated and experimental stress-strain responses of heat treated the Al3003 sheet at 500°C for 1hr

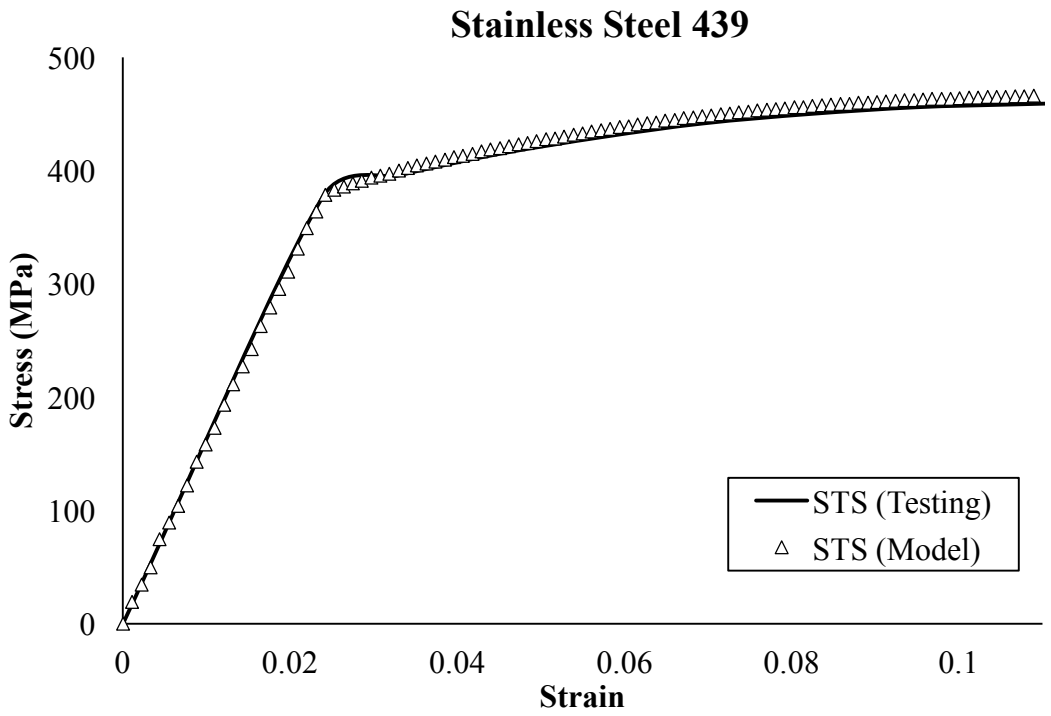

Figure 9. Simulated and experimental stress-strain responses for the Stainless Steel 439 sheet at 500°C for 1hr

2.5.4 Contour profiles at select increments

Figure 10 shows the Cauchy stress tensor components of an infinitesimal three-dimensional rectangular element. The coordinate system is defined as (1,2,3) to correspond with that defined in Abaqus. The contour plot of STS 439 is shown in **Figure 11** to exemplify the stress distribution throughout the prismatic specimen in the elastic region, yield and at the ultimate point in the y direction of the specimen. The legend shows the stress profile of the specimen in the y-direction, defined as S22 as per the coordinate system shown in **Figure 10**.

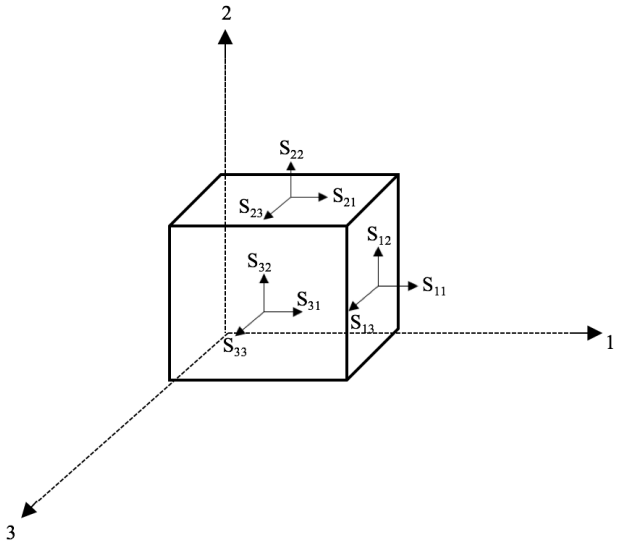

Figure 10: Three-dimensional Cauchy stress tensor components

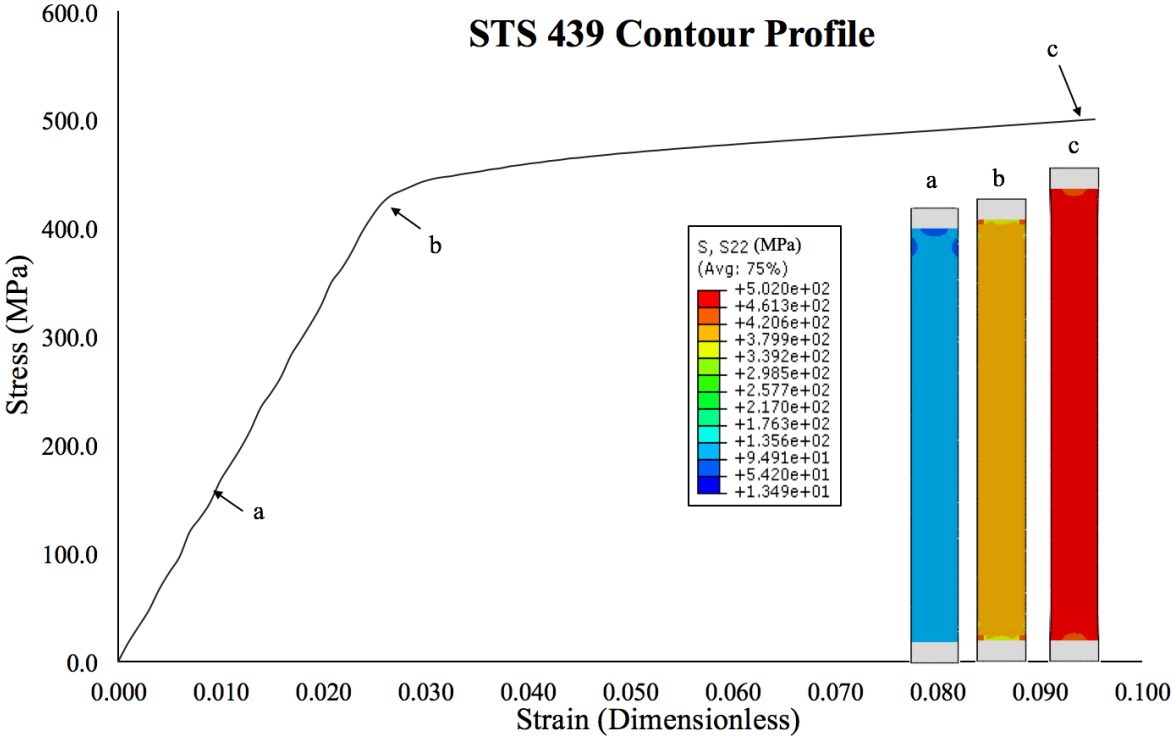

Figure 11: STS 439 stress-strain curve and typical contour profile in S22 direction of specimen

2.5.5 Implementation of the model to simulate the individual component tensile deformation characteristics of a tri-layered composite

Another journal publication by Kim and Hong (2013) investigated the mechanical behavior of a tri-layered magnesium AZ31, aluminum 3004, and Cr ferritic stainless steel 430 cladded sheet. The thicknesses of the testing layered sheets are 0.5 mm, 1 mm, and 2.3 mm for stainless steel (SST430), aluminum (Al3004), and magnesium (AZ31), respectively. The gauge length and width of the specimen are 15 mm and 3.4 mm, respectively. The specimen was heat-treated at 673°K for 3 hrs.

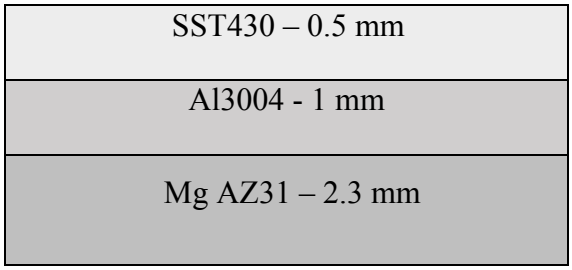

Figure 12. Arrangement and dimensions of layered plates: AZ31 Mg/3004 Al/SST 430 used by Kim and Hong (2013)

A tensile test was conducted on the separate and combined materials, which generated corresponding stress-strain responses. The model was applied using the same procedure as described in the previous sections, but with adjusted thickness dimensions. The generated output stress-strain response can be seen in **Figures 13-15**. These testing and simulated stress-strain responses are compared below for each separate material. The

combined materials will be discussed in **Chapter 3**.

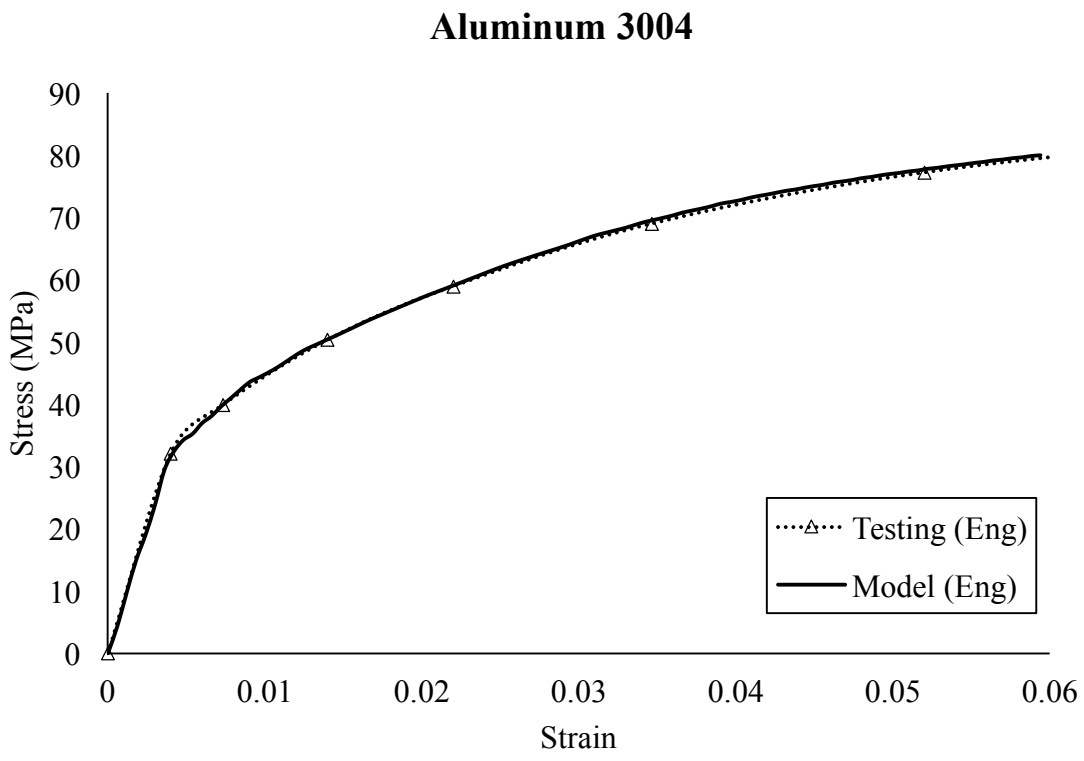

Figure 13. Simulated and experimental stress-strain responses for the Al 3004 sheet at 673°K for 3 hrs.

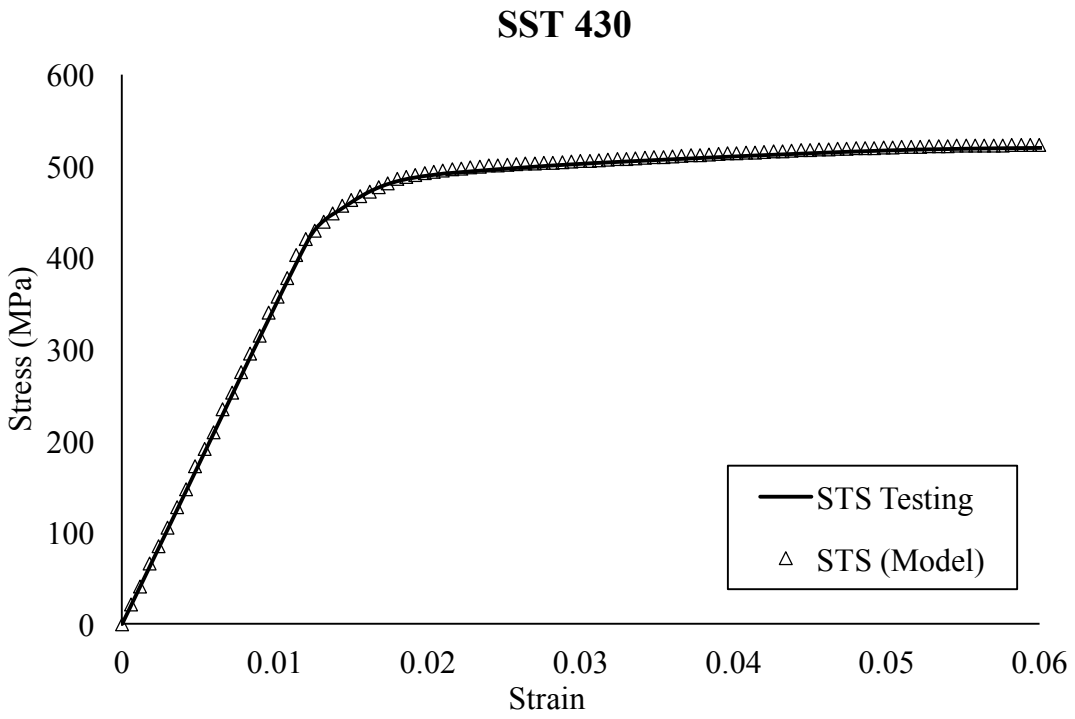

Figure 14. Simulated and experimental stress-strain responses for the Stainless Steel 430 sheet at 673°K for 3 hrs.

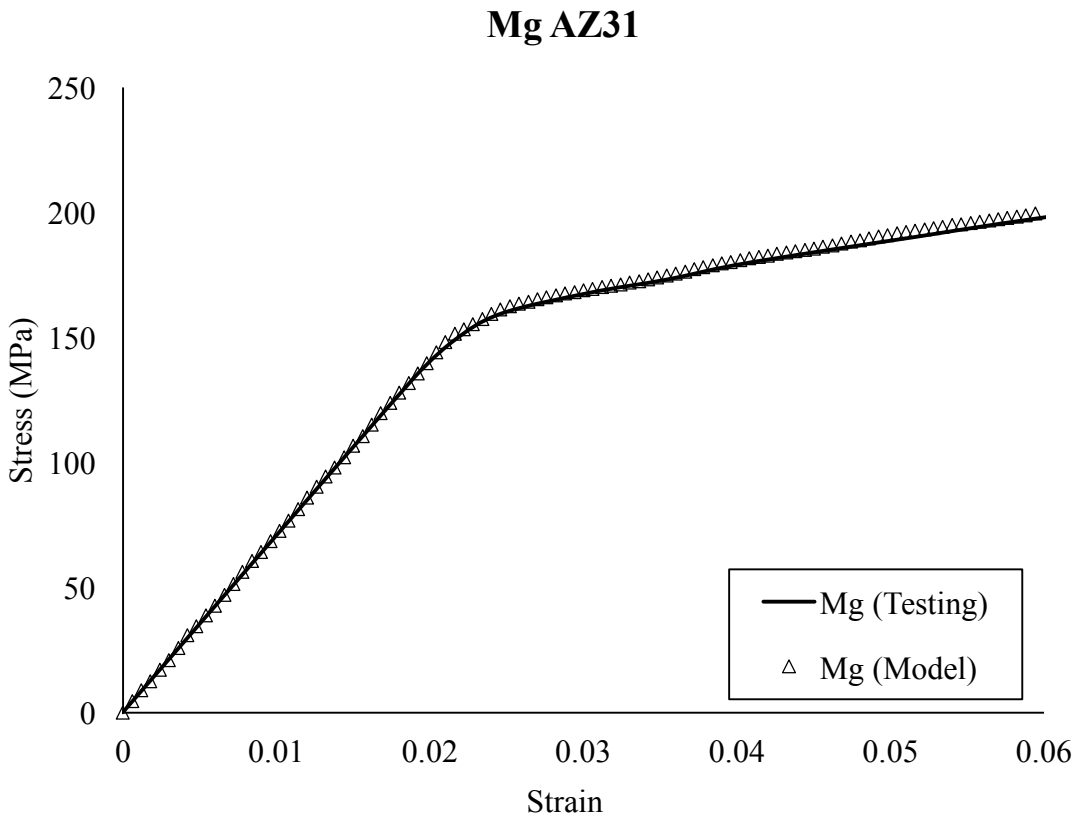

Figure 15. Simulated and experimental stress-strain responses for the Magnesium AZ31 sheet at 673°K for 3 hrs.

2.6 Comparisons of Simulation and Experimental Behaviors

Table 1 compares the yield and tensile properties of the experimental results and those derived analytically. The percent difference was below 1.2 % for all experimental and simulated values. The similarity of these comparisons confirms the model's effectiveness in predicting the mechanical properties of materials. Moreover, the model's proficiency in verifying mechanical properties supports its claim of accuracy. The outcome of these comparisons demonstrates that the model serves to provide substantiated results and can

efficiently predict the mechanical behavior of any composite comprising of previously evaluated materials. All materials are added to an embedded material library within Abaqus to be made available for future use.

Table 1. Comparison of experimental and simulated yield and tensile properties

Property	Material				
	Al 3003	STS 439	Al 3004	SST 430	AZ31
Experimental Yield Strength, σ_{Yexp} (MPa)	49.0	377.4	32.1	419.4	133.3
Simulated Yield Strength, σ_{Ymod} (MPa)	48.5	378.3	32.4	420.4	133.4
% Difference (Yield)	**1.02**	**0.238**	**0.93**	**0.24**	**0.07**
Experimental Ultimate Strength, σ_{ULexp} (MPa)	94.6	460.7	79.8	520.3	201.3
Simulated Ultimate Strength (MPa), σ_{ULmod}	94.3	466.2	80.2	523.3	200.2
% Difference (Ultimate)	**0.32**	**1.18**	**0.50**	**0.57**	**0.55**

2.7 Ramberg-Osgood parameters

The Ramberg-Osgood (R-O) material constants of Aluminum 3003 and Steel 439 were obtained using a trial-and-error curve fitting method using **Equation 1.13**. The reason for selecting the standard Ramberg-Osgood formula is explained in the literature review, **Section 1.4**. The ultimate purpose of employing the R-O method is to reaffirm the

model's accuracy. The standard form of the R-O formula denoted in **Section 1.2.6** was used to determine the constants of (n-1) and α using excel.

The E, α, σ_0, and (n-1) parameters were adjusted until matching curves were achieved at various experimental and modeled heat-treated temperatures. The experimental stress-strain responses obtained from Jin and Hong (2013) matched well with those determined analytically using the standard R-O equation. The R-O curves were also a good fit with the modeled stress-strain responses, thereby indicating that the model falls into an excellent margin of accuracy. The closely matching representative curve seen in **Figure 16** below compares the curve obtained using the R-O relationship to the experimentally obtained response at a heat treatment temperature of Steel 439 at 400°C.

Table 2 below compares the experimental and modeled R-O constants to demonstrate their close proximity to one another.

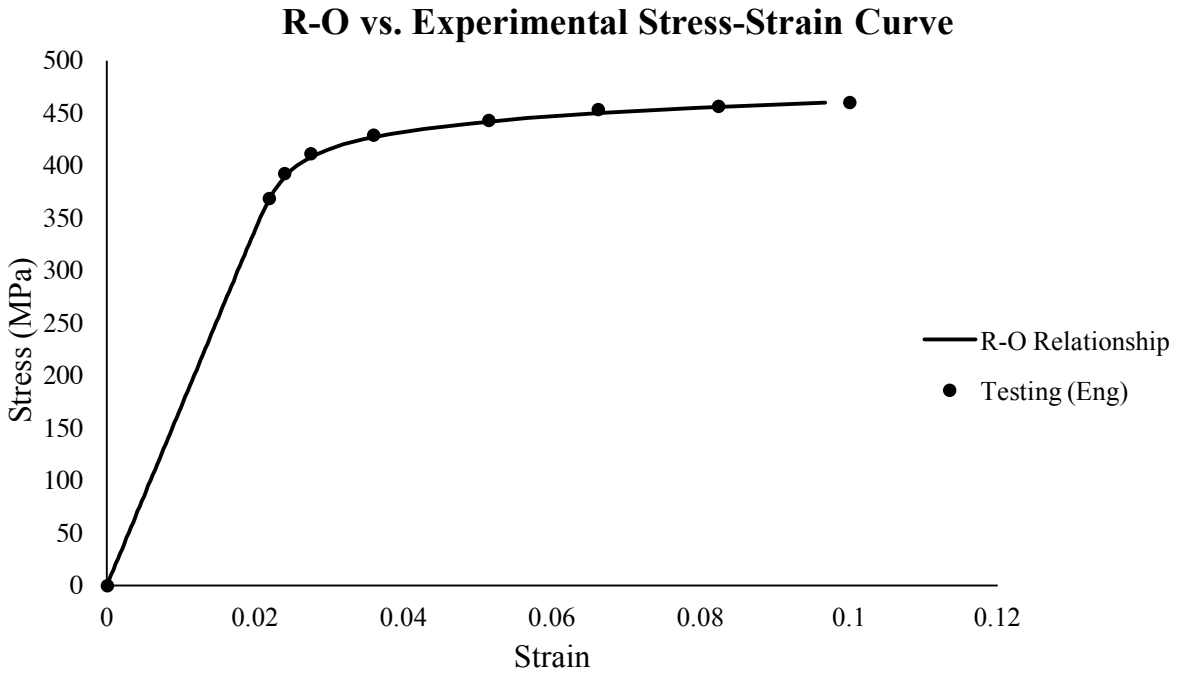

Figure 16: Comparison of the R-O and testing stress-strain curves of Steel 439 at 400C

Table 2: R-O parameters of experimental and modeled stress-strain responses of Al 3003 at various temperatures

Al 3003	As-rolled		200°C		300°C		400°C		500°C	
	EXP	Model	EXP	Model	EXP	Model	EXP	Model	EXP	Model
E (MPa)	3550	3600	3500	3500	3200	3150	2950	3000	3100	3150
α	0.11	0.11	0.09	0.1	0.11	0.1	0.1	0.1	0.09	0.1
σ_0	127	130	111	114	69	70	69	70	49	50
(n-1)	22	22	21	21	9.7	9.7	9.3	9.5	6.25	6.1

Table 3: R-O parameters of experimental and modeled stress-strain responses of STS 439 at various temperatures

STS 439	As-rolled		200°C		300°C		400°C		500°C	
	EXP	Model	EXP	Model	EXP	Model	EXP	Model	EXP	Model
E (GPa)	15.6	16.25	17.0	16.7	18.3	18.5	17.0	16.9	16.0	16.0
α	0.15	0.14	0.13	0.13	0.09	0.09	0.09	0.08	0.07	0.06
σ_0	423	426	420	427	417	423	400	406	360	360
(n-1)	35	34	32	32	28	28	25	25	16.5	16

2.8 Conclusions

The high volume of allocated time and resources in laboratory testing indicates an inherent need for numerical modeling to enhance productivity. Laboratory testing of large-scale applications such as aircrafts or vessels is challenging. Numerical modeling is a promising approach to studying the mechanical behavior of composites by separately investigating its component materials. The complexities associated with modeling composites can be remedied by predicting the stress-strain response of its component materials. The following conclusions are based on the modeling results of the individual materials and their comparisons with experimental data:

- The confidence of the model's accuracy is displayed by its ability to generate simulated stress-strain responses, which are in close agreement with those of testing. Studying the interaction of component materials is useful to predict the behavior of the overall composite. This model can be extended to simulate stress-stress responses of composites discussed in the following chapter.

- The tensile tests conducted by Jin and Hong (2013) and by Kim and Hong (2013) generated stress-strain responses for each of the composite's separate and combined materials, which were then compared to the model's output responses within the elastic-plastic region of the curve to coincide with the scope of this thesis. The model's output stress-strain response is valid regardless of geometry based on the mathematical definition of engineering stress-strain. The initial modulus of elasticity was calculated after converting the true stress-strain data to engineering stress-strain.
- The Ramberg-Osgood (R-O) relationship was used to verify the accuracy of the model. The R-O parameters were obtained through curve fitting and were found to match closely to both the experimental and modeled stress-strain responses.
- Investigating the tensile deformation at any given cross-sectional area is significant and innovative because it allows the model to provide more flexibility to investigate the elastic-plastic behavior of larger-scale specimens. Since most material testing is limited to small-scale specimens, extending this FEM model to predict material behavior in large-scale specimens without the need to conduct large-scale testing could potentially save an immense amount of time and resources. In brief, comparing the testing and simulated stress-strain responses efficiently simulates material behavior without accumulating any associated costs or resources. This model's accuracy was verified by equating a series of simulated stress-strain curves against those of testing. Ultimately, this model provides an excellent feasibility study because it can apply previously obtained results from

less costly small-scale testing to predict a material's performance on a large-scale structure, such as in an aircraft. This FE model's well-developed technique can be extended to efficiently model the mechanical properties of composites, which will be discussed in the following chapter.

2.9 References

Aakash, B.S, Connors, JohnPatrick, and Shields, Michael D. "Stress-strain Data for Aluminum 6061-T651 from 9 Lots at 6 Temperatures under Uniaxial and Plane Strain Tension." Data in Brief 25 (2019): 104085.
Ambriz, R. R., C. Froustey, and G. Mesmacque. "Determination of the tensile behavior at middle strain rate of AA6061-T6 aluminum alloy welds." International Journal of Impact Engineering 60 (2013): 107-119.

Bobbili, Ravindranadh, Madhu, Vemuri, and Gogia, Ashok Kumar. "Tensile Behaviour of Aluminium 7017 Alloy at Various Temperatures and Strain Rates." Journal of Materials Research and Technology 5.2 (2016): 190-97.

Chen, Y, Clausen, A.H, Hopperstad, O.S, and Langseth, M. "Stress–strain Behaviour of Aluminium Alloys at a Wide Range of Strain Rates." International Journal of Solids and Structures 46.21 (2009): 3825-835.

Elruby, Ahmed Y, and Nakhla, Sam. "Strain Energy Density Based Damage Initiation in Heavily Cross-linked Epoxy Using XFEM." Theoretical and Applied Fracture Mechanics 103 (2019): 102254.

Elruby, A Y, and Nakhla, Sam. "Extending the Ramberg–Osgood Relationship to Account for Metal Porosity." Metallurgical and Materials Transactions. A, Physical Metallurgy and Materials Science 50.7 (2019): 3121-131.

Gao, Xiaosheng, Zhang, Tingting, Hayden, Matthew, and Roe, Charles. "Effects of the Stress State on Plasticity and Ductile Failure of an Aluminum 5083 Alloy." International Journal of Plasticity 25.12 (2009): 2366-382.

Jain, M, Allin, J, and Lloyd, D.J. "Fracture Limit Prediction Using Ductile Fracture Criteria for Forming of an Automotive Aluminum Sheet." International Journal of Mechanical Sciences 41.10 (1999): 1273-288.

Jin, Ju Young, and Hong, Sun Ig. "Effect of Heat Treatment on Tensile Deformation Characteristics and Properties of Al3003/STS439 Clad Composite." Materials Science & Engineering. A, Structural Materials: Properties, Microstructure and Processing 596 (2014): 1-8.

Kim, In-Kyu, and Hong, Sun Ig. "Roll-Bonded Tri-Layered Mg/Al/Stainless Steel Clad Composites and Their Deformation and Fracture Behavior." Metallurgical and Materials Transactions. A, Physical Metallurgy and Materials Science 44.8 (2013): 3890-900.

Ramberg, Walter, and William R. Osgood. "Description of stress-strain curves by three parameters." (1943).

Yandt, S., P. Au, J-P Immarigeon, Xj. Wu, Wu, XJ., American Society for Testing Materials, and ASTM International. Modeling Thermomechanical Cyclic Deformation by Evolution of Its Activation Energy. 2003.

Zhao, Xuehang, Li, Haifeng, Chen, Tong, Cao, Bao'an, and Li, Xia. "Mechanical Properties of Aluminum Alloys under Low-Cycle Fatigue Loading." Materials 12.13 (2019): 2064.

3 FEA of the Elastoplastic Behavior of Multilayered Clad Composites

3.1 Introduction

Numerically modeling the behavioral response of composites provides an innovative solution to a magnitude of structural applications. Numerically modeling composites is sparsely available in the literature, with a predominant focus on punch tests and forming limit diagrams to determine behavioral responses. Yilamu et al. (2009) employed the Yoshida-Uemori model to determine the springback based on bending angle calculations. Jain et al. (1998) conducted a FE simulation to determine the ductile fracture using forming limit diagrams to predict failure during stamping. Unlike the previous chapter, this section considers the behavior of the composite as a whole. This chapter presents a unique and transcending finite element model to determine the mechanical behavior of composites under uniaxial tensile loading.

3.2 Modeling Procedure for Composite Material Assembly

The results in **Chapter 2** confirmed the model's validity by generating modeled results that were within a range of 1.5% accuracy compared to the results obtained through testing. The model can therefore be extended to embody multilayered composite materials. The model geometry can be modified to include several materials layers. Each layer is assigned its corresponding material properties and thickness. Several parts consisting of different materials and thicknesses can be modeled together as a single composite using the assembly function.

As previously mentioned, all materials in **Chapter 2** were added to an embedded material library for ease of access. A material library affords significant flexibility to create modeled composites. Saving materials within a library allows a more efficient analysis because repeatedly redefining is often time-consuming and increases human error potential. The Al3003/STS430 and Mg AZ31/Al 3004/SST439 clad composites were created in Abaqus using the assembly function. The desired materials were selected from the material library to be analytically bonded together to form the two composites, as shown in **Figure 17**.

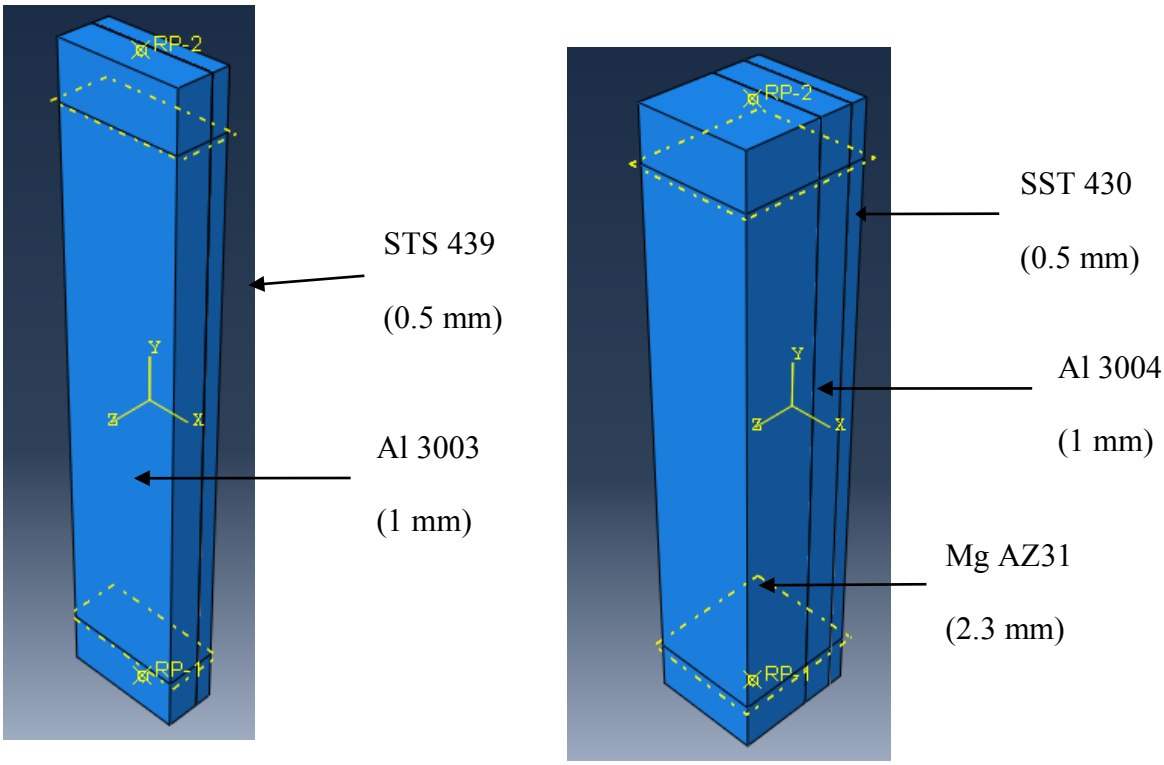

Figure 17. Modeled geometry of Al3003/STS439 and Mg AZ31/Al3004/SST430 clad composites

The Al3003/STS439 modeled geometry adopts the gauge width and length from the initial testing. The length is 15 mm, and the width is 3.5 mm. The thickness of Al3003 and STS439 are 1 mm and 0.5 mm, respectively. As shown in **Figure 16**, Al3003 and STS439 are modeled as individual parts. A mesh of 0.5 was used (based on the results of a mesh convergence study) for both the aluminum and steel parts. The Mg AZ31/Al3004/SST430 roll bonded tri-layered composite has a gauge length and width of 15 mm and 3.4 mm, respectively. The assembly function combined the desired materials into a composite by importing materials from the Abaqus material library. The interaction between the two sheets is defined as a tie (surface to surface). Once the composite was completed, the same technique conducted for the individual materials was applied to generate the stress-strain response.

3.3 Simulation Results and Discussion

Figure 18 demonstrates the experimental and modeled stress-strain responses for both the Al3003/STS439 clad composite. The modeled output response coincides with that of testing. The agreement of the responses suggests that there existed little interference within the interfacial layer of the aluminum and steel.

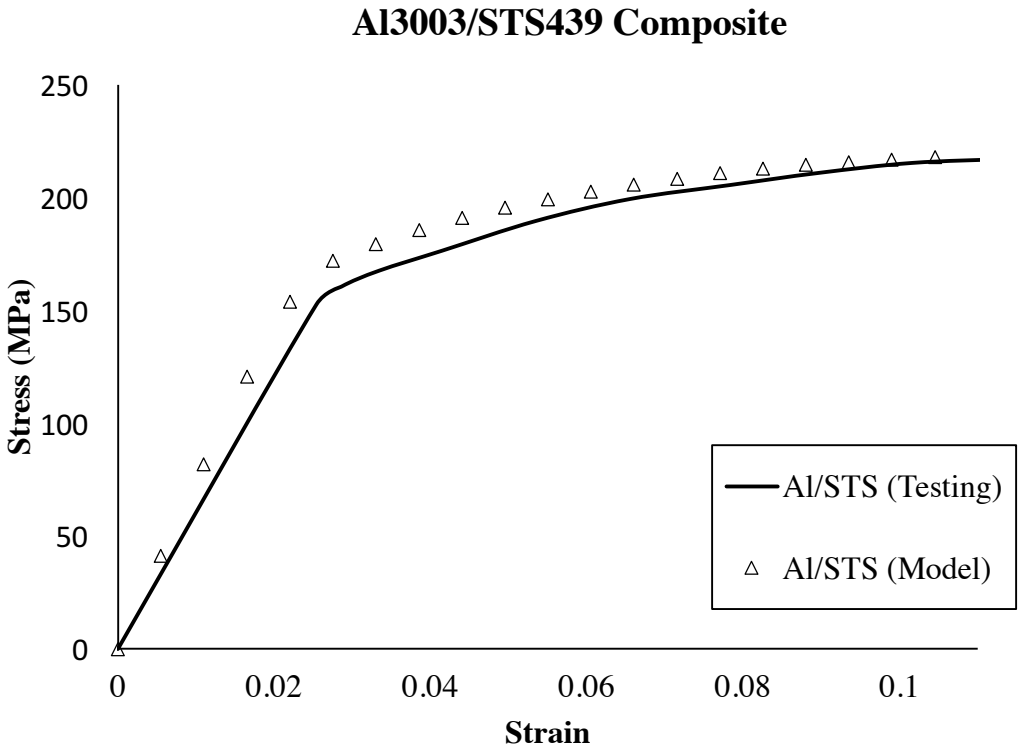

Figure 18. Simulated and testing engineering stress-strain response comparison for Al3003/STS439 clad composite.

3.4 Mesh convergence study for Al3003-STS439 clad composite

The purpose of a mesh convergence study is to determine an adequate mesh size that poses no influence on the results of an analysis. Defining the required number of elements within a mesh is accomplished by generating a series of curves with different mesh sizes and examining any corresponding changes in the results. The number of elements in a mesh are increased until the mesh eventually converges to an optimal element size and produces repeatable results. To elaborate, the adequate mesh size is established once the solution is no longer affected despite a further increase to the number of elements.

A mesh convergence study was performed on the Al3003-STS439 clad composite to determine an adequate mesh size to implement into the model's FE analysis. Stress-strain curves were generated using mesh sizes of 1.5 mm, 1 mm and 0.5 mm. **Figure 19** reveals almost identical stress-strain responses for each of the aforementioned mesh sizes. The mesh size converged to 0.5 mm, after which there was found to be no significant difference in solution.

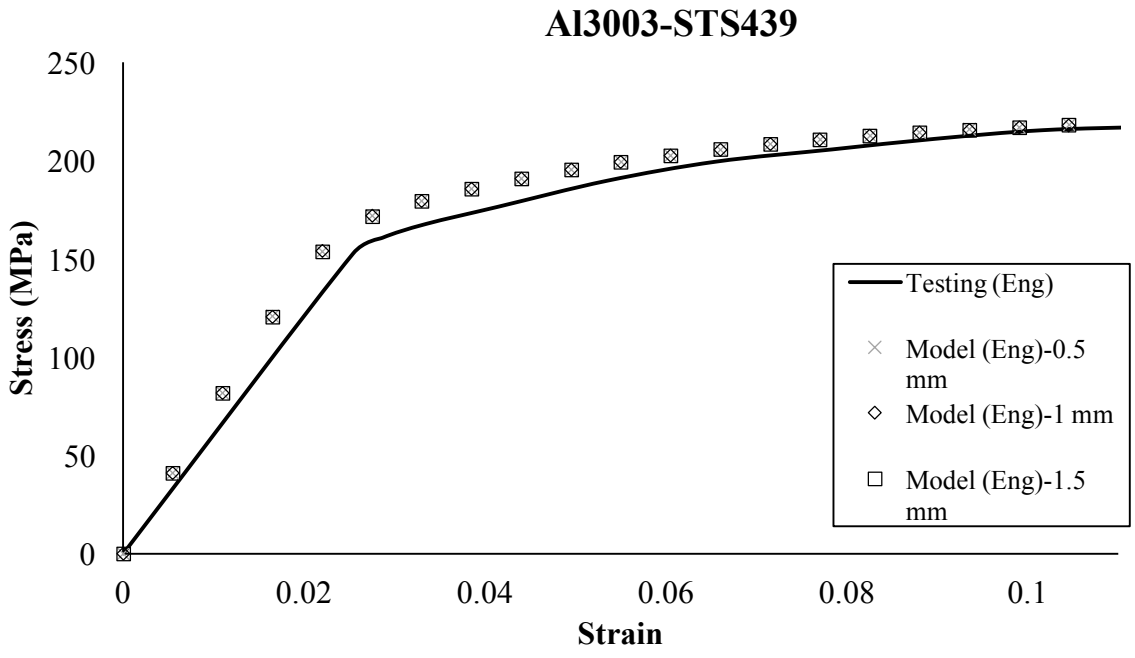

Figure 19: Stress-strain responses of mesh convergence study at mesh sizes of 0.5 mm, 1 mm, and 1.5 mm

Figure 20 provides a detailed summary of the mechanical responses for the individual and combined materials for the Al3003/STS439 composite. As expected, the composite's mechanical behavior falls in between those of its contributing materials.

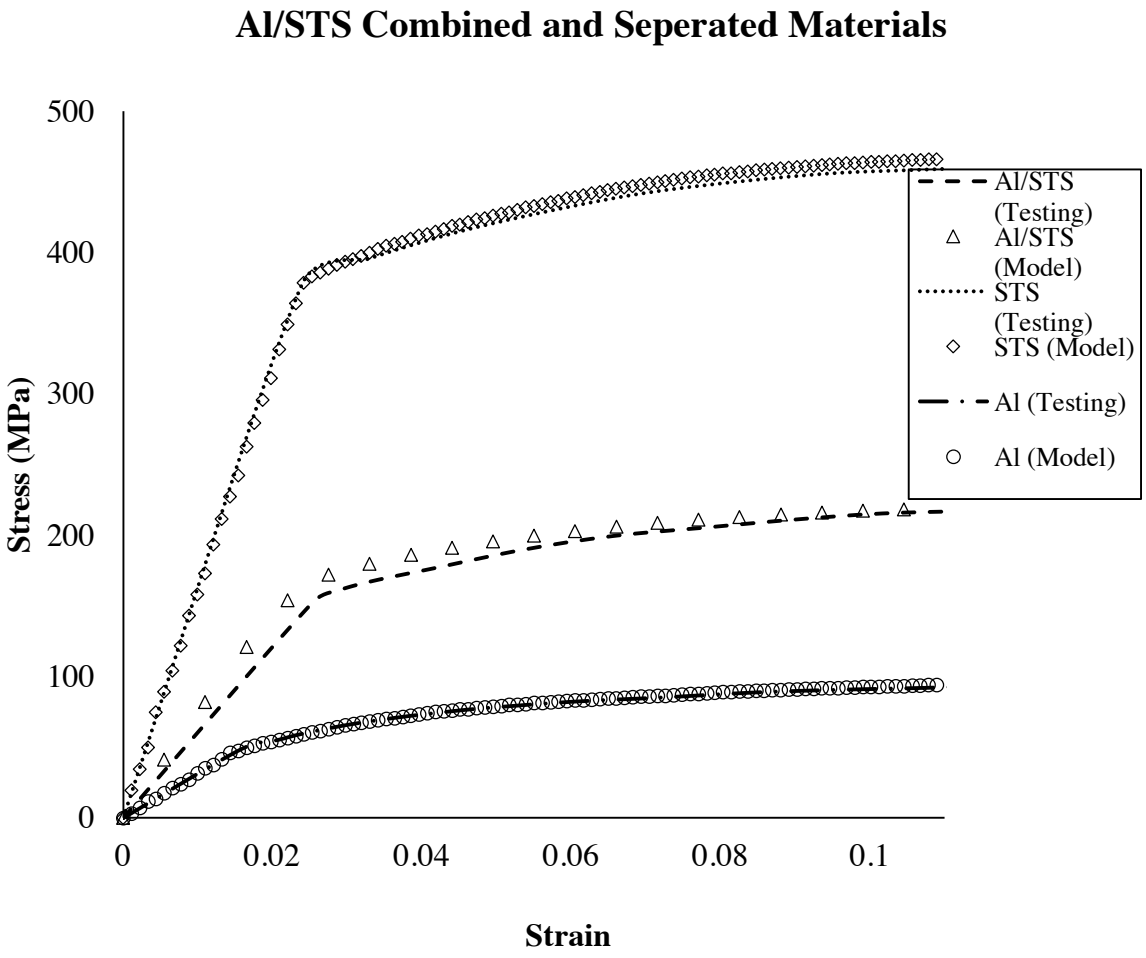

Figure 20. Comparison of modeled and simulated engineering stress-strain responses of individual and combined materials within the composite

Figure 21 shows the mechanical response for the combined and separate contributing materials for the MgAZ21/Al3004/SST430 composite. The modeled response differs

slightly from that of testing, indicating a disturbance within the reaction layer. The development of a thin passive film on the Mg/Al interface region was observed in the optical micrographs, with the intermetallic compounds of $A_{l3}Mg_2$ and $Al_{12}Mg_{17}$ (Kim and Hong, 2013).

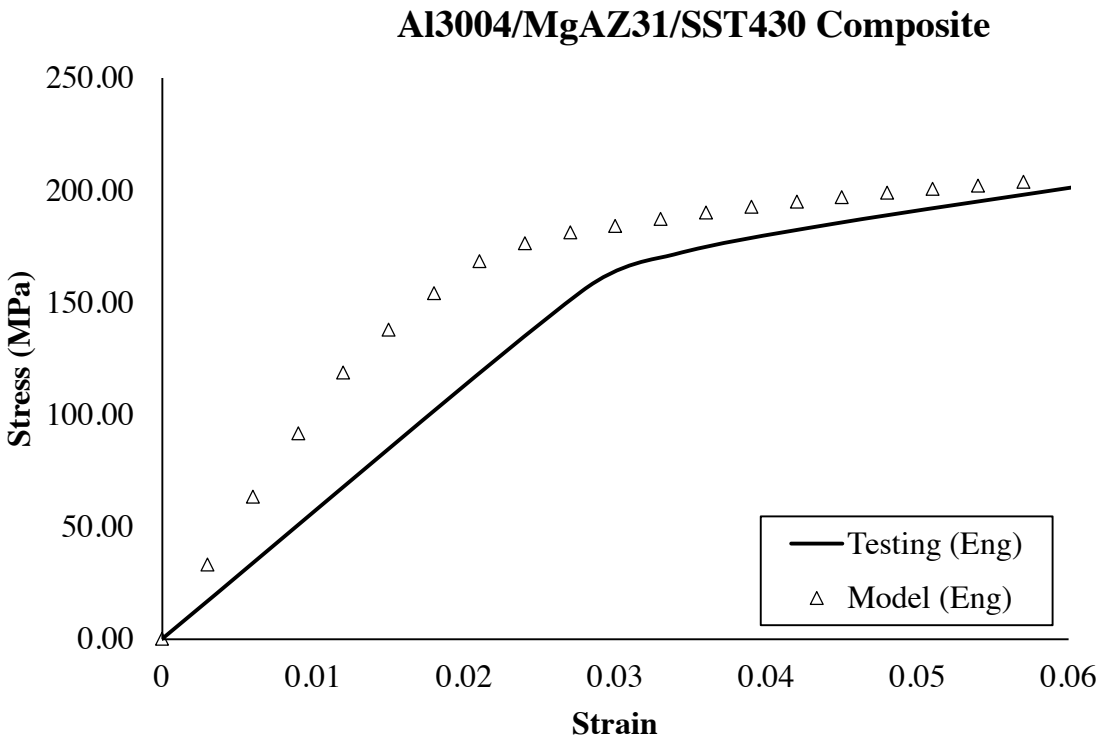

Figure 21. Simulated and testing stress-strain response comparison of Al3004/MgAZ31/SST430 composite

Figure 22 shows the stress-strain responses for the MgAZ31/Al3004/SST430 composite and all separate contributing materials. The composite's response behaves very similarly to Mg alone, which the authors interpreted to mean that this material combination offers no advantage to be used in structural applications (Kim and Hong, 2013). The authors

suggested that cladding magnesium with steel might offer a more feasible result. Experimentally investigating the stress-strain response of a new composite would require an entirely new tensile experiment despite comprising of the same materials. Roll bonding the materials and then subjecting them to a new tensile test is time-consuming and accumulates costs associated with laboratory resources. The following chapter extends the designed FE model to predict the exact material arrangement suggested by the authors: the mechanical behavior of a magnesium and steel-clad composite. In this way, the feasibility of combining these materials results could be presented without any additional costs. Young's Modulus is an important parameter used to describe the elastic performance of a material. Young's Modulus was tabulated from the stress-strain curves and used as an input parameter to define the elastic behavior of the modeled materials.

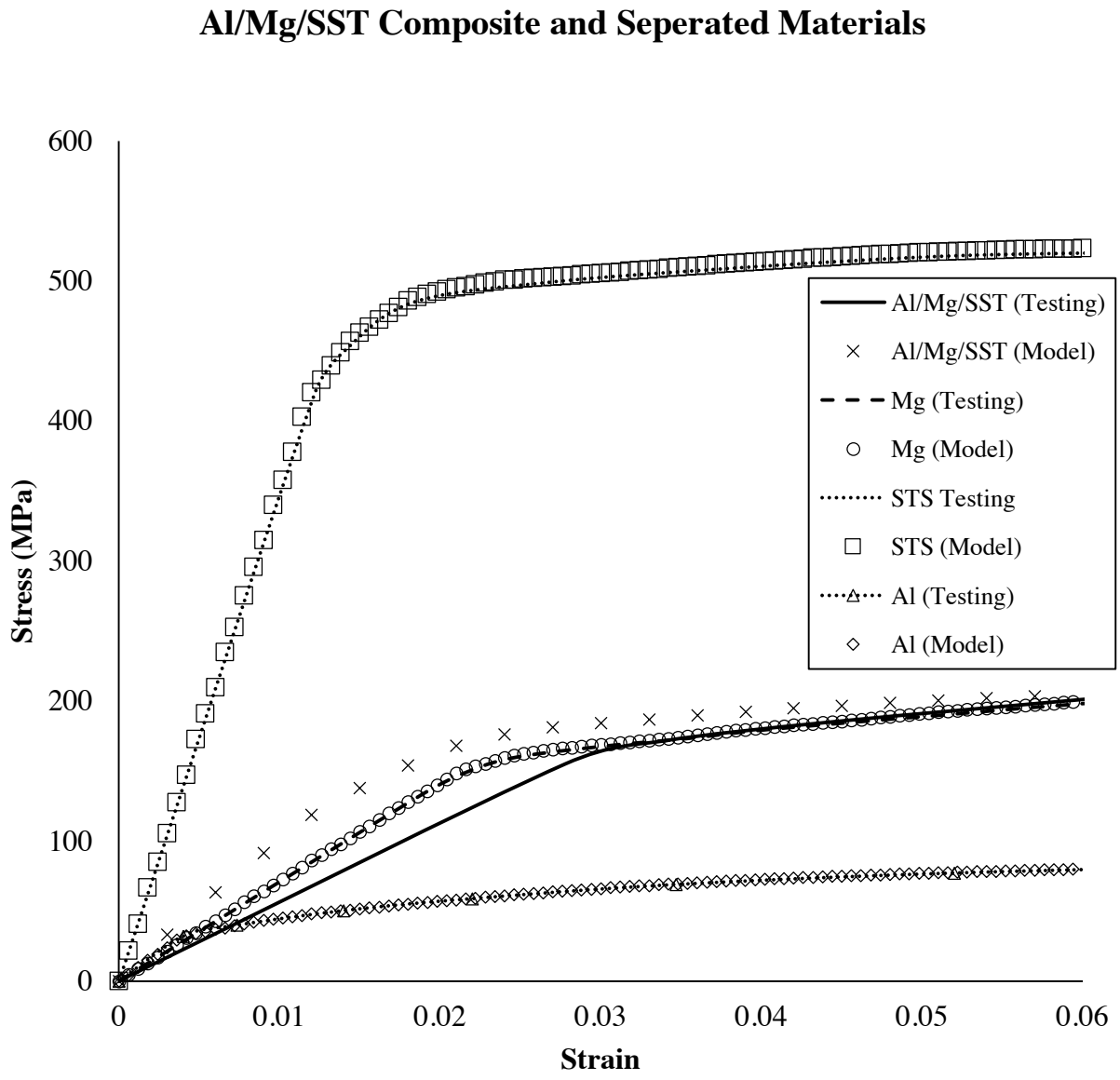

Figure 22. Simulated and testing stress-strain response comparison of Al3004/MgAZ31/SST430 composite and individual component materials

3.5 Comparisons of Simulation and Experimental Behaviors

Table 4 provides a clearer perspective on the above stress-strain responses. The percent difference for the yield strength is slightly higher than the ultimate strength. This difference could be attributed to hindrances in the interfacial layers, in agreement with an observed growth of a passive film seen in the optical micrographs of Kim and Hong (2013). However, the percent difference of the ultimate tensile strength is below 1%. This model contributes significantly to predicting the ultimate tensile strength of composites.

Table 4. Summary of simulated and testing mechanical responses

Property	Material	
	Al3003/STS439	Al3004/SST430/AZ31
Experimental Yield Strength, σ_{Yexp} (MPa)	152.8	154.9
Simulated Yield Strength (MPa), σ_{Ymod}	165.2	173.4
% Difference (Yield)	**7.5**	**10.7**
Experimental Ultimate Strength (MPa), σ_{ULexp}	217.3	203.0
Simulated Ultimate Strength (MPa), σ_{ULmod}	218.4	205.0
% Difference (Ultimate)	**0.50**	**0.98**

3.6 Conclusions

The flexibility of customizing composites using previously defined material properties and geometry saves time and resources. The simulated and experimental stress-strain responses of composites were compared to determine the feasibility of applying this model to composites. The percent difference for the yield strengths Al3003/STS439 and Mg/Al3004/SST430 were 10.7% and 7.5%, respectively. The percent difference between the simulated and testing ultimate strengths were less than 1% for both composites. The reasoning for the slightly larger discrepancy in yield strength could be attributed to flaws within the interfacial layers. Despite the uncertainty surrounding the potential imperfections within the interfacial layers, this model provides accurate and consistent values and can therefore be extended to model composites with modified attributes using previously determined material properties, such as Young's Modulus, elastic and plastic behavior, etc.

3.7 References

Ha, Jong Su, and Hong, Sun Ig. "Design of High Strength Cu Alloy Interlayer for Mechanical Bonding Ti to Steel and Characterization of Their Tri-layered Clad." Materials in Engineering 51 (2013): 293-99.

Hong, Sun Ig, and Kim, Yong Keun. "Residual Stress/Strain Effect on the Bending Properties of the Cu/Al/Cu Clad Plate." Key Engineering Materials 737 (2017): 214-19.

Kim, In-Kyu, and Hong, Sun Ig. "Roll-Bonded Tri-Layered Mg/Al/Stainless Steel Clad Composites and Their Deformation and Fracture Behavior." Metallurgical and Materials Transactions. A, Physical Metallurgy and Materials Science 44.8 (2013): 3890-900.

Kim, In-Kyu, and Hong, Sun Ig. "Roll-Bonded Tri-Layered Mg/Al/Stainless Steel Clad Composites and Their Deformation and Fracture Behavior." Metallurgical and Materials Transactions. A, Physical Metallurgy and Materials Science 44.8 (2013): 3890-900.

Li, Xiaobing, Zu, Guoyin, and Wang, Ping. "Effect of Strain Rate on Tensile Performance of Al/Cu/Al Laminated Composites Produced by Asymmetrical Roll Bonding." Materials Science & Engineering. A, Structural Materials: Properties, Microstructure and Processing 575 (2013): 61-64.

Morovvati, Mohammad Reza, Morovvati, Mohammad Reza, Fatemi, Afshin, Fatemi, Afshin, Sadighi, Mojtaba, and Sadighi, Mojtaba. "Experimental and Finite Element Investigation on Wrinkling of Circular Single Layer and Two-layer Sheet Metals in Deep Drawing Process." International Journal of Advanced Manufacturing Technology 54.1 (2011): 113-21.

Zhu, Deju, Mobasher, Barzin, Rajan, S. D, and Peralta, Pedro. "Characterization of Dynamic Tensile Testing Using Aluminum Alloy 6061-T6 at Intermediate Strain Rates." Journal of Engineering Mechanics 137.10 (2011): 669-79.

4 Modeling Composite Candidates: A Parametric Study

4.1 Introduction

Composite modeling provides an excellent tool for feasibility studies coupled with significant decreases in resources. Creating a material library using behavioral responses from experimental data delivers substantial advancements in composite modeling. Contrary to laboratory tensile tests that require physical resources, FEMs allow virtual modifications and trials to be conducted until the optimal composite design is achieved. The purpose of these simulations is to provide a parametric study of composite designs from a library of materials verified with experimental data. The finite element model analysis outputs the mechanical response of the newly created composites to provide a yield and ultimate strength comparison. These comparisons are tremendously resourceful to determine the feasibility of their potential structural applications because they reveal which paired materials function best cladded together. The model's convenience is embedded within its versatility and accuracy, which are compelling motives for industrial applications.

4.2 Modeling the Behavior of Clad Composite Candidates

The previous chapters explain the verification process to determine the FEM's accuracy of generating reliable stress-strain responses. The following parametric studies implement the FEM to simulate the mechanical behavior of composite candidates. The selected thicknesses of all sheet layers remain the same as the original experiment to provide a fitting analysis to the original authors' assumption. The composite candidates are compared in **Figure 23** to illustrate the influence the composition of a composite's material has on yield and ultimate strength.

4.2.1 Candidate 1: MgAZ31/SST430 Clad Composite

A magnesium and stainless steel-clad composite is modeled using materials from the material library created within Abaqus. These particular component materials are selected in accordance with the suggestion mentioned by Kim and Hong (2013). Their work determined that cladding magnesium, aluminum, and stainless steel provided no added benefit but stated that a Mg/SST composite could potentially provide more optimal results. The implementation of a parametric simulation for Mg/SST generated a behavioral response with a higher yield and ultimate strength than that of the initial tri-layered composite, which therefore supports the authors' hypothesis.

4.2.2 Candidate 2: Al3004/SST430 Clad Composite

The aluminum stainless steel-clad composite candidate was simulated to strengthen the soundness of the parametric study. Illustrating the response for the Al3004/SST430 provides additional comparative data to ensure the consideration of all possible design aspects. The Al3004/SST430 composite candidate revealed a higher yield and ultimate strength than the initial composite, as shown in **Figure 23**.

4.3 Clad Composite Candidates Discussion and Comparisons

Although both candidates showed enhanced mechanical behavior compared to the original composite, they each provide different advantages that need to be considered based on the eventual design's indented purpose. Despite having the higher tensile strength, MgAZ31/SST430 generated a response with a slightly lower yield strength than that of the Al3004/SST430 composite candidate. **Table 5** summarizes the yield and ultimate strengths for all composite candidates. The highest yield and tensile strengths are bolded for clarity.

Table 5. Summary of yield strength and ultimate strength of composite candidates

Property	Material		
	MgAZ31/Al3004/SST430	MgAZ31/SST430	Al3004/SST430
Yield Strength (MPa)	118.7	146.6	**189.0**
Ultimate Strength (MPa)	205.0	**259.2**	228.4

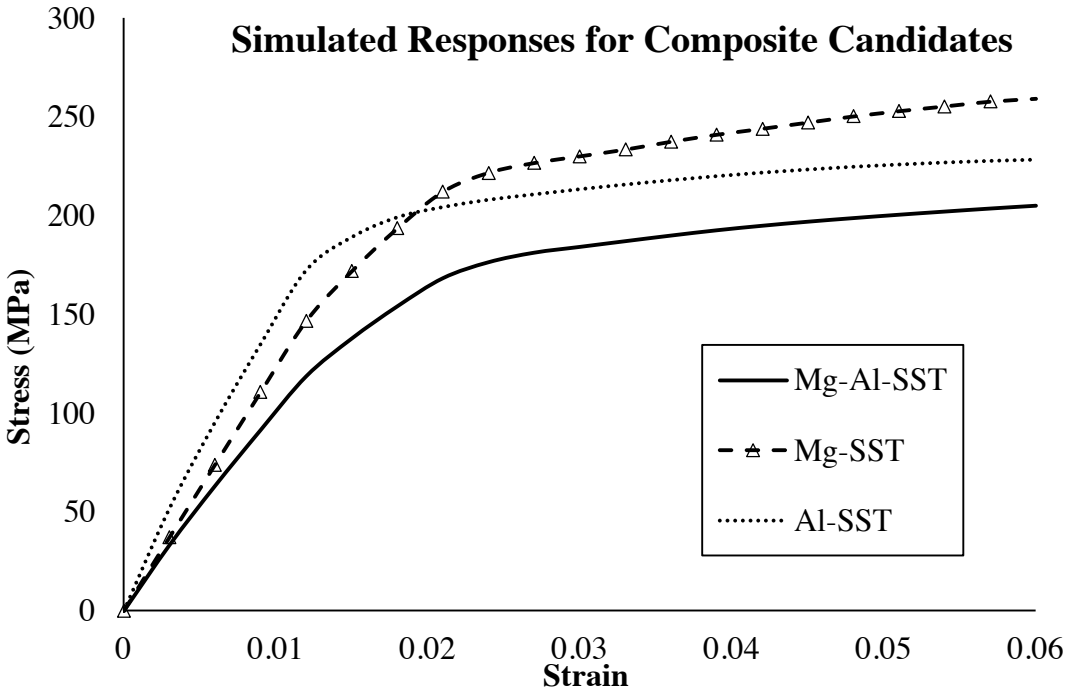

Figure 23. Comparative stress-strain responses of composite candidates

4.4 Conclusions

The suggestion proposed by Kim and Hong (2013) of cladding stainless steel to magnesium was investigated using a parametric study. The parametric study revealed the stress-strain responses of the composite candidates of MgAZ31/SST430 and Al3004/STS430 each demonstrated higher yield and ultimate values. The purpose of this parametric study was to provide a comparative analysis to facilitate future informed decisions on designing an optimal candidate based on the indented function.

Instead of conducting a new set of experiments to predict a composite's behavior, the FE model can be modified to effectively determine the behavioral response of material candidates without requiring costs associated with multiple laboratory testing. The same reasoning could be applied to exploring the behavior of any composite. Rather than conducting tensile tests on several composite candidates to search for an optimal behavioral response, this model could instead be used to estimate the behavioral response and determine its feasibility. Experimental testing could proceed on the most optimal candidate to lessen the number of experiments required to determine an optimal composition, saving both time and resources. Experimenting on a composite only to determine that it may not be optimal for an intended use falls short of a solution. Experimentally testing optimized composite candidates suggested by the model's output mechanical behavior provides a more educated decision and could mitigate the costs associated with testing numerous unsuccessful composite compositions. A modeled simulation provides simulated stress-strain responses that can be used to determine the feasibility of considering an ideal and superior composite candidate for an experiment.

4.5 References

Eff, Michael N. “A Fundamental Investigation into Intermetallic Formation and Growth in the Aluminum-Iron System Using Resistance-Based Diffusion Couples” (2019).

Jeong, H. T., & Kim, W. J. (2020). “Strain hardening behavior and strengthening mechanism in mg-rich Al–Mg binary alloys subjected to aging treatment.” Materials Science & Engineering.A, Structural Materials: Properties, Microstructure and Processing, 794, 1.

Jin, Ju Young, and Hong, Sun Ig. "Effect of Heat Treatment on Tensile Deformation Characteristics and Properties of Al3003/STS439 Clad Composite." Materials Science & Engineering. A, Structural Materials: Properties, Microstructure and Processing 596 (2014): 1-8.

Kang, G. T., Song, J. S., & Hong, S. I. (2017). “Effect of roll-bonding temperature on the strength and electrical conductivity of an alpha -brass-clad cu-1Cr alloy composite.” Physics of Metals and Metallography, 118(2), 190-197.

Kim, In-Kyu, and Hong, Sun Ig. "Roll-Bonded Tri-Layered Mg/Al/Stainless Steel Clad Composites and Their Deformation and Fracture Behavior." Metallurgical and Materials Transactions.” A, Physical Metallurgy and Materials Science 44.8 (2013): 3890-900.

Kim, Hyung Jin, Kim, Hyung Jin, Hong, Sun Ig, and Hong, Sun Ig. "Effect of Ni Interlayer on the Interface Toughening and Thermal Stability of Cu/Al/Cu Clad Composites." Metals and Materials International 25.1 (2019): 94-104.

Liu, Bert C. "Joining dissimilar structural alloys by vaporizing foil actuator welding: process conditions, microstructure, corrosion, and strength." PhD diss., The Ohio State University, 2016.

Volokitina, I E, and Volokitin, A V. "Evolution of the Microstructure and Mechanical Properties of Copper during the Pressing–Drawing Process." Physics of Metals and Metallography 119.9 (2018): 917-21.

Zhang, Rui, Wang, DongJun, Liu, ShiQiu, Ding, HongSheng, and Yuan, ShiJian. "Effect of Microstructures on Hot Compression Behavior of a Ti-43Al-2Si Alloy Fabricated by Cold Crucible Continuous Casting." Materials Characterization 144 (2018): 424-30.

5 Summary and Conclusions

5.1 Summary

A literature review comprising of the behavior of multilayer and clad composites was presented in the first chapter. An explanation of the FE model's implementation was proposed and verified in the second chapter, with particular attention given to a composite's component materials' behavioral response and mechanical properties. The Ramberg-Osgood relationship was used to confirm the model's accuracy by generating stress-strain responses that were in close agreement with that of the modelled curve along with the original experimental data. The third chapter explores the model's capability to be extended further by simulating the behavioral response for a composite as a whole (combined contributing layers) using Abaqus' assembly function. The fourth chapter offers a parametric study for two composite candidates to illustrate the capacity of the model's versatility to compute results without amassing a considerable amount of resources.

5.2 Contributions

This thesis's contributions are immense for the primary purpose of providing a low-cost solution to optimize composite material candidates. Implementing the FE model allows users to explore composite designs using modified materials, sequences, and geometry. The implementation of this model can be extended to accurately predict the mechanical behavior of composites within an acceptable range without the lengthy and costly process of laboratory testing. Applications include accurately simulating numerous composite compositions to present several options which can be used to make informed decisions on selecting fewer composite candidates for a reduced number of laboratory trials.

5.3 Recommendations for Future Work

This section identifies the shortcomings of this model and proposes potential solutions. The simulated yield strength of composites occupies the least accurate percent difference. As previously mentioned, the interfacial layers of neighboring materials may form passive films. Modeling composites without considering the effects of interfacial layers between metals generates a less accurate stress-strain response. Certain limitations exist when modeling composites compared to individual materials. Such can be seen in **Figure 21**, which shows that the model's stress-strain response of the composite is not as close as that of testing despite the individual material simulated and testing responses being very similar. Future research could introduce numerical modeling of the vulnerabilities present within the interfacial layers of clad composites. A solution for modeling the vulnerabilities of interfacial layers could potentially reduce the percent difference range of the simulated and experimental yield strength.